Cdc14 phosphatase ensures resolution of aberrant meiotic recombination outcomes partly through activating Yen1/GEN1

Carolina Pascual-Silva,[1,¶] Katerina Strouhalova,[1,¶] George B. Garside,[2,¶] Meret Arter,[3] David Álvarez-Melo,[1] Teresa Bermejo,[1] Pedro San-Segundo,[4] Joao Matos,[3] Marco Geymonat,[5] Jesús A. Carballo[1,*]

[1] Department of Cellular and Molecular Biology, Centro de Investigaciones Biológicas CSIC, Ramiro de Maeztu 9, 28040, Madrid, Spain

[2] Leibniz Institute for Age Research/Fritz Lipmann Institute (FLI) Beutenbergstr. 11; D-07745 Jena; Germany

[3] Institute of Biochemistry, HPM D6.5 - ETH Zürich, Otto-Stern-Weg 3, 8093 Zürich, Switzerland

[4] Instituto de Biología Funcional y Genómica. Consejo Superior de Investigaciones Científicas and University of Salamanca. 37007-Salamanca, Spain

[5] Department of Genetics, University of Cambridge, Downing Street, Cambridge, CB2 3EH, United Kingdom

¶ These authors contributed equally to this work

*Corresponding author: j.carballo@cib.csic.es

Abstract

Meiotic defects derived from incorrect DNA repair during gametogenesis can lead to mutations, aneuploidies and infertility. Effective and coordinated resolution of meiotic recombination intermediates is necessary to accomplish both rounds of successful chromosome segregation. Cdc14 is an evolutionarily conserved dual-specificity phosphatase required for mitotic exit and meiotic progression. Mutations that inactivate the phosphatase lead to meiotic failure. Here, we have identified previously unseen roles of Cdc14 in ensuring correct meiotic recombination. We found that aberrant recombination intermediates accumulate during prophase I when Cdc14 protein levels are drastically reduced. Furthermore, Cdc14 plays a role in suppressing the formation of non-allelic (ectopic) recombination products. We also demonstrate that Cdc14 is required for correct sister chromatid disjunction during the second meiotic divisions. Finally, Cdc14 is required in meiosis for the timely activation of the conserved Holliday Junction resolvase, Yen1/GEN1 in anaphase II. Based on these new findings we propose an early function for Cdc14 in meiotic recombination independent of its later roles during anaphase I/II.

Author Summary

Meiotic recombination is fundamental for sexual reproduction, effective and coordinated resolution of recombination intermediates is critical for correct chromosome segregation. Homologous recombination is initiated by the introduction of programmed DSBs followed by the formation of complex branched DNA intermediates, including double Holliday Junctions (dHJs). These recombination intermediates are eventually repaired into crossover or non-crossover products. In some cases, unresolved recombination intermediates, or toxic repair products, might persist until the metaphase to anaphase transition, requiring of a subset of late-acting repairing enzymes to process them. Unrestrained activity of these enzymes might equally put at risk the genome integrity, thus, several layers of regulation tightly control them. For example, in budding yeast meiosis, Yen1/GEN1 is only activated during the second meiotic division, although how it is activated is unknown. Here, we have identified the requirement of the Cdc14 phosphatase for the timely activation of Yen1 during the second division in meiotic cells. Additionally, we have been able to identify a previously undescribed role of Cdc14 in meiotic recombination. Strikingly, we found that levels of aberrant recombination intermediates accumulate during prophase I in *cdc14* meiotic deficient cells. Furthermore, in the absence of Cdc14 activity, there is an increase of ectopic recombination products, indicating that Cdc14 plays a direct role in monitoring meiotic DSB repair, possibly in a way independent of Yen1. Such accumulation of persistent recombination intermediates is not sensed by the checkpoint machinery at the end of prophase I, and their abnormal accumulation in *cdc14* meiotic cells likely contribute to the missegregation problems observed during the second meiotic division.

Introduction

Meiotic recombination is initiated by the conserved Spo11 transesterase, which introduces numerous DNA Double-Strand Breaks (DSBs) into the genome [1]. Association of single strand DNA binding proteins, including RPA, Rad51 and the meiosis specific recombinase, Dmc1, to the resected DSB ends promotes strand invasion into the intact homologous non-sister chromatid template, which culminates with the formation of a displacement loop (D-loop). Nascent D-loops can be processed through the Synthesis Dependent Strand Annealing (SDSA) repair pathway to generate non-crossover (NCO) repair products [2]. Alternatively, stabilization of the D-loop followed by second-end capture give rise to double Holliday Junction (dHJ) intermediates. In budding yeast meiosis, dHJs are most frequently resolved into crossovers (COs) through the combined action of Mlh1-Mlh3 (MutLγ) and Exo1 [3,4]. A second class of COs arises from the resolution of recombination intermediates via the Structure Specific Endonuclease (SSE) Mus81/Mms4 [5]. In addition, when both 3'-ends of the DSB, invade two different repair templates, three and four interconnected duplexes, also known as multichromatid joint molecules (mc-JMs), can be observed [6]. Further, both 3'-ends might also participate in multi-invasion events onto two or three chromatids, creating heavily branched DNA structures [7]. These complex DNA

species must be efficiently processed at risk of becoming potential hazards for the genome integrity due to their capacity to form aberrant crossovers, or other forms of toxic repair products. Resolution of mc-JMs molecules requires the orchestrated action of a set of helicases and endonucleases, capable of displacing multi-branched DNA assemblies. The Bloom's syndrome helicase (BLM/Sgs1), in addition to be involved in SDSA repair, it plays a prominent role in resolving aberrant "off-pathway" JMs, including mc-JMs [8-12].

It is less clear what enzymatic complexes take over the function of removing any unresolved branched DNA intermediate, once meiotic cells leave the pachytene stage. Upon activation of *NDT80*-dependent transcription, and activation of the budding yeast polo-like kinase Cdc5, cells abandon the pachytene stage concomitantly with a surge of enzymatic activity that culminates with the resolution of ZMM-stabilized dHJs to form IH-COs and NCOs [13,14]. Cdc5 phosphorylation is required to activate a set of Structure-Specific Endonucleases (SSEs), most notoriously Mus81-Mms4 [15]. Mus81-Mms4 complex acts over branched DNA substrates that have not been resolved by the canonical, ZMM-interfering COs pathway [4,10]. On the other hand, Yen1^{GEN1}, a conserved member of the Rad2/XPG family of SSEs, including a number of proteins involved in DNA replication, recombination and repair; appears to act much later in meiosis, in spite of the fact that Yen1 is considered a prototypical HJ resolvase [16]. In meiotic cells, this discrepancy is easily explained, since the activity of Yen1 is negatively regulated by CDK-dependent phosphorylation, precluding the nuclease to act during prophase I [15]. Abolition of CDK-phosphorylation in Yen1, turns on the protein's enzymatic activity as well as promotes its nuclear localization, leading to the conclusion that counteracting the phosphorylation of Yen1 brings about the nuclease activity into its fully functional form [15,17]. In mitotic cells, dephosphorylation of Yen1 is carried out by the Cdc14 phosphatase [18,19]. Activation of Yen1 during anaphase by Cdc14 allows the resolution of persistent repair intermediates that otherwise impose a physical impediment to chromosome segregation. It is currently unknown whether Cdc14 also dephosphorylates Yen1 in meiosis. Furthermore, it is unclear whether Yen1 might be activated following anaphase I onset, or it is limited to anaphase II exclusively [4,15].

Cdc14 is a well-conserved dual-specificity phosphatase, and it has been defined as a key component in the reversal of CDK phosphorylation during the completion of mitosis [20]. In budding yeast, Cdc14 activity is essential, and cells lacking this phosphatase will remain arrested at the end of mitosis [21,22]. Several pathways regulate Cdc14 localization and activity. The RENT complex, required for transcription inhibition at the rDNA intergenic spacers (IGS), retains Cdc14 at the nucleolus until anaphase through its interaction with the Cif1/Net1 protein [23,24]. Additionally, Cdc14 regulates transcriptional silencing at the rDNA, and other repeated sequences, [25-27]. Cdc14 is released from the nucleolus by the sequential action of two additional pathways. The FEAR (Cdc Fourteen Early Anaphase Release) pathway promotes the early release of Cdc14 through the phosphorylation of Cif1/Net1 and Cdc14 [28-33]. Late in anaphase, the Mitotic Exit Network (MEN) keeps Cdc14 in its

released state, allowing the de-phosphorylation of additional substrates, important for the full termination of mitosis and cytokinesis [34,35].

In addition to curtail CDK activity at the end of mitosis, Cdc14 plays critical roles promoting chromosome segregation [36]. In *S. cerevisiae*, it is required for the correct segregation of the ribosomal gene array (rDNA) and telomeres [37-39]. Lack of transcriptional silencing at these regions prevents the loading of condensins at the rDNA, and subtelomeric regions [27,37,40], which leads to unresolved linkages, intertwined sister chromatids, and non-disjunction during mid-anaphase. Notably, a number of functions have been allocated to Cdc14 before its anaphase-triggered release. In particular, Cdc14 has been involved in completion of late-replicating regions in the rDNA, and other parts of the genome [41]. Another anaphase-independent release of Cdc14 was observed upon induction of DNA damage, where generation of DSBs promoted the transitory release of Cdc14 out of the nucleolus, targeting the SPB component Spc110 for dephosphorylation [42].

Cdc14 is also critically required for the completion of meiosis [43]. In budding yeast, Cdc14 is released from the nucleolus in two waves; the first during anaphase I, and a second in anaphase II [44-46]. Contrary to mitotic cells, Cdc14 release from the nucleolus requires the essential function the FEAR pathway whereas it appears that the MEN pathway is dispensable [47-49]. Additionally, some components of the MEN pathway, such as Cdc15, have functionally differentiated to fulfil a requirement in spore morphogenesis [47,48]. Meiotic depletion of the MEN component Cdc15 leads to progression through both meiotic divisions but impairs spore formation. Such differentiated function of Cdc15 in meiosis appears to be independent of Cdc14 [48]. Curiously, inactivation of the FEAR pathway in meiosis allows exclusively one meiotic division to take place, culminating with the formation of asci carrying two diploid spores (dyads) [44,45,47,50,51].

Premature activation of FEAR blocks spindle assembly during meiosis, a process normally averted by $PP2A^{Cdc55}$ [52-54]. On the other hand, inactivation of Cdc14 function by means of FEAR mutants, or by employing conditional temperature sensitive alleles of the phosphatase, blocks meiosis once the first division has been completed [44,45]. Furthermore, absence of the phosphatase creates chromosome entanglements, a problem that can be reverted by deleting *SPO11* [45]. Nonetheless, the absence of Cdc14 activity does not always prevent the disassembly of the meiosis I spindle upon completion of anaphase I, and *cdc14* cells carry out MII-like divisions utilizing the existing MI-spindle [53]. These interesting observations prompted the identification of another critical function of Cdc14 during meiosis I to meiosis II transition, which is the re-licensing of SPBs in order to re-assemble functional meiosis II spindles. Asymmetrical enrichment of Cdc14 on a single SPB during anaphase I promotes SPB re-duplication, otherwise preventing the initial step of morphogenesis of new SPBs [55].

Cdc14 is highly conserved and orthologues have been identified in other organisms, including, fission yeast, nematodes, insects, and vertebrates [56]. The human genome contains three Cdc14 homologues, hCDC14A, hCDC14B and hCDC14C [57,58]. Depletion of Cdc14A, required for mitotic CDK inactivation, leads to defects in centrosome duplication, mitosis and cytokinesis [59]. In vertebrates,

CDC14B exit the nucleolus in response to DNA damage [60,61], a process conserved in fission yeast [62], and more recently observed also in budding yeast [42]. Thus, in addition to play important roles in the DNA Damage Response (DDR) [60] it appears that both Cdc14A and Cdc14B might be required for efficient repair of damaged DNA [61].

Here, we describe various previously unknown roles of Cdc14 in budding yeast's meiosis. First, we reveal its direct involvement in ensuring correct meiotic recombination by suppressing the formation of non-allelic (ectopic) recombination products. We also show that Cdc14 functions in resolving a subset of aberrant JMs, presumably by regulating other substrates during, or concomitantly with, the completion of prophase I. Finally, we demonstrate that Cdc14 is required for the timely activation of the conserved HJ resolvase, Yen1/GEN1 at anaphase II. *cdc14* mutants, defective in those previously uncharacterized functions, display extensive chromosome non-disjunction and aneuploidies.

Results

cdc14^{3HA} is a novel meiosis-specific separation-of-function allele of *CDC14*

During the course of previous unrelated studies, we generated the *cdc14^{3HA}* allele carrying an endogenous C-terminal tagged version of the *CDC14* gene with three copies of the hemagglutinin epitope (3HA).

Unlike other temperature sensitive alleles of *cdc14* used in many studies (see introduction), mitotic growth was not affected in diploid cells carrying the *cdc14^{3HA}* allele when grown at different temperatures on solid or liquid media (Fig 1A; data not shown). Thus, we concluded that *cdc14^{3HA}* cells behave like *CDC14* at all temperatures tested under our standard unchallenged growth conditions.

Unexpectedly, when homozygous SK1 background diploid *cdc14^{3HA}* cells were induced to sporulate in liquid media, very few asci that contained spores were visualized. In contrast, *CDC14* control strains analyzed in parallel showed extensive formation of tetrads (asci containing four spores) (Fig 1B). Following an extended incubation time in sporulation media, cells with untagged and tagged Cdc14 were sampled at 24, 48, 72, or 96 hours, fixed and analyzed under the microscope. Over 90% of cells in the *CDC14* diploid completed sporulation after 24 hours (Fig 1B). Conversely, *cdc14^{3HA}* strains displayed as few as 10% of asci containing one or two spores at all times examined (Fig 1B).

To confirm the observed defect in liquid media during sporogenesis of *cdc14^{3HA}* cells, we further induced sporulation in solid media and assessed the presence of N,N-bisformylldityrosine in the sporulated cultures. Dityrosine is a component that comprises approximately 50% of the mass of the outer spore wall layer [63]. Dityrosine is an autofluorescent molecule that possesses an excitation and emission wavelength of 325nm and 400nm respectively. Thus, when sporulated cultures are exposed under the UV^{325nm} light, spores emit visible light that can be detected using standard photographic methods (Fig 1C). *CDC14* and *cdc14^{3HA}* cells were plated at three different dilutions on sporulation media and they were incubated for at least three days. Following that incubation time, plates were

directly illuminated with both white light, and UV light and they were photographed (Fig 1C, top and bottom panel respectively). As anticipated, control wild-type diploid strains induced to sporulate emitted light at a wavelength of 400nm after irradiation with UV light. On the other hand, *cdc14*^{3HA} diploid colonies did not emit light at the 400nm wavelength after irradiation with UV light (Fig 1C). All together, we confirm that *cdc14*^{3HA} diploid strains cannot complete sporulation despite their apparently normal mitotic growth.

Bulk DNA synthesis is not altered in *cdc14*^{3HA} mutant cells

To get further insights into the underlying causes by which *cdc14*^{3HA} mutants fail to sporulate, we followed different stage-specific markers to characterize in detail its phenotype.

First, we sought to find whether the initiation of the meiotic program was altered by studying meiotic DNA replication kinetics. During the mitotic cell cycle, released Cdc14 has been shown to de-phosphorylate some replication factors, including Sld2 and Dpb2 [64]. In addition, the lack of Cdc14 activity has been linked to problems during DNA replication termination [41]. Thus, we studied the possibility that affecting the regulatory circuit involving the Cdc14 phosphatase could cause bulk DNA replication problems during meiotic S-phase. We found that S-phase progressed at nearly identical kinetics in both control and *cdc14*^{3HA} strains (Fig 1D). This result suggests that initiation of meiotic S-phase is not altered in *cdc14*^{3HA} cells and that the bulk of the DNA completes replication within the same kinetics as the wild type.

cdc14^{3HA} cells initiate both meiotic divisions

In most organisms, meiosis is characterized by a single round of DNA replication followed by two rounds of nuclear divisions [65], thus we examined whether *cdc14*^{3HA} cells were capable of separating the nuclear content during both meiotic divisions. To achieve that, synchronous cultures of *CDC14* and *cdc14*^{3HA} were run in parallel and samples were collected and fixed every two hours for at least 10-12 hours and up to 24 hours. Fixed samples were stained with 4',6-diamidino-2-phenylindole (DAPI) and counted under the fluorescence microscope for nuclear division. Results showed that *CDC14* cells initiated nuclear divisions around five hours after their transference into sporulation media and most cells displayed more than one DAPI-stained nucleus by ten hours (Fig 1E). On the other hand, *cdc14*^{3HA} cells displayed subtly slower kinetics of nuclear divisions as well as a lower amount of cells exiting the one-nucleus stage by ten hours. Prolonged time-courses showed that, eventually, most *cdc14*^{3HA} cells exited the one nuclei stage, although with a two-hour delay with respect to *CDC14* control cells (not shown).

Previous work has shown that temperature sensitive mutants of *cdc14* arrest following anaphase I completion with two nuclei, due to those cells being unable to assemble functional meiosis II spindles [43,45,53,66]. Furthermore, in the very few cells that continue to the second round of chromosome

segregation in *cdc14 ts* mutants, MII spindle does not form properly, because of problems in SPB reduplication/half-bridge separation during meiosis I to meiosis II transition [55]. SPB half-bridge separation likely requires the de-phosphorylation by Cdc14 of the SPB component Sfi1 during anaphase I [67]. We noticed, however, that nuclear divisions went past the two-nuclei stage in *cdc14*^{3HA} meiotic cells (S1A Fig), distinguishing this 3xHA C-terminal tagged version of the Cdc14 phosphatase from those temperature sensitive alleles described in earlier studies.

Cdc14 protein levels are depleted during meiosis in *cdc14*^{3HA} cells

To discern the cause of the phenotype of *cdc14*^{3HA} strains we analyzed Cdc14^{3HA} protein levels during the entire length of our meiotic time-courses. *CDC14* and *cdc14*^{3HA} cells were synchronized and induced to sporulate in parallel. Samples were collected every 2 hours and protein extracts obtained from each sample. Western blot analysis showed that, *cdc14*^{3HA} cells accumulate reduced levels of the tagged protein, even at time zero, prior to meiotic induction. Levels of Cdc14^{3HA} protein become untraceable following the initiation of the meiotic time course, quite more significantly at times matching the end of meiotic S-phase and beginning of prophase I (Figs 2A and 1D). Currently, it is unknown to us what triggers this selective and abrupt protein degradation process of the Cdc14^{3HA} phosphatase. We exclude the nature of the tag itself, as Smk1-3HA protein was included as internal control in our western blots, and proteins levels were stable, and even increased during mid to late meiosis (Fig 2A). Overproduction of the Cdc14^{3HA} protein restored the sporulation defect, as well as increasing the copy number of different *cdc14* alleles (S2 Fig). These results confirm that meiosis-specific depletion of the Cdc14^{3HA} protein is causing the sporulation defect. Additional biochemical and structural studies might be required to unveil the reason of this protein degradation phenotype, which appears to be more drastic in meiotic cells.

Meiotic *cdc14*-deficient cells undergo two rounds of SPB duplication/separation to eventually degenerate

Once identified what the cause of the meiotic phenotype of *cdc14*^{3HA} cells was, we proceeded to study at the cellular and molecular level what might be preventing *cdc14*^{3HA} cells from completing sporulation when the protein levels of the phosphatase are depleted. As mentioned above, most *cdc14*^{3HA} cells eventually went past the two-nuclei stage observed as terminal meiotic phenotype in other *cdc14* temperature sensitive mutants [43,45,66]. Thus, we monitored the kinetics and morphology of the meiotic SPBs and spindles during the first and the second divisions. Both *CDC14* and *cdc14*^{3HA} cells, carrying GFP-tubulin and Spc29-CFP to visualize spindles and SPBs, respectively, were induced to undergo synchronous meiosis. Samples were then collected and studied under the microscope at times where MI, MII, and later stages in the sporogenic process take place [68-70]. In addition to the kinetics of nuclear divisions, the number of SPBs per individual cell were counted. Cells with two or more

Spc29-CFP foci were considered to have initiated one or both meiotic divisions (Fig 2C-D; S3A Fig). This was confirmed by the presence of linearly distributed bundles of microtubules characteristic of the meiotic spindle (Fig 2C). Furthermore, nuclear segregation was monitored simultaneously by looking at the separation of SPB-associated DAPI masses (Fig 2D). We observed that by eight hours into meiosis, *CDC14* and *cdc14*^{3HA} cultures contained around 75% and 60% of cells with more than one SPB, respectively. Among the population of cells that showed multiple SPBs, 56% of wild-type cells presented more than two Spc29 foci; therefore, they had initiated meiosis II. However, only 40% of *cdc14*^{3HA} cells displayed more than two Spc29 foci, confirming a slight reduction of cells forming meiosis II spindles carrying four SPBs. This observation correlates with the slightly lower frequency of *cdc14*^{3HA} cells containing more than two DAPI masses (Fig 2D; S1A Fig). As expected, after 24 hours of meiotic induction, wild-type *CDC14* cells showed over 90% of cells with three or four SPBs. In marked contrast, the *cdc14*^{3HA} meiotic mutant presented more than two thirds of the cells lacking a single Spc29-CFP focus, suggesting that, in the absence of Cdc14, the structural integrity of SPBs becomes compromised once meiotic divisions take place (Fig 2D; S3 Fig).

Meiotic spindle dynamics are not altered in the *cdc14*^{3HA} mutant

Since we found that SPB re-duplication was not impeded in the *cdc14*^{3HA} mutant, along with the fact that we could detect cells past the second nuclear division, we investigated whether the observed SPBs assembled functional spindles at both MI and MII. In addition, we assessed if the kinetics of both chromosomal divisions were altered in the mutant. To test that, wild-type and *cdc14*^{3HA} strains carrying Tub1-GFP and Spc29-CFP were induced to undergo meiosis synchronously and at appropriate times, they were transferred to an incubator chamber for image acquisition using live-cell microscopy (Fig 3A-B). To analyze meiosis I division, time between metaphase I and the end of telophase I was recorded. Thus, for *CDC14* cells, the MI spindle extension-to-breakage period lasted around 53 min under our experimental conditions. Cells from the *cdc14*^{3HA} culture completed MI in 58 min (Fig 3C). Despite of this six minutes delay in the absence of *cdc14*^{3HA} mutant, the differences were not statistically significant. Next, we estimated the length of MII by timing the period between metaphase II spindles followed by the lengthening of the microtubule bundles until the tubulin signal became diffuse (Fig 3B). Average length of MII divisions was 80 min and 86 min for *CDC14* and *cdc14*^{3HA} cells, respectively (Fig 3C), also for this case not significantly different. Taken together, we conclude that the detected reduction in Cdc14 abundance throughout meiosis does not affect the lifespan of either meiotic I, or meiotic II spindles.

Missegregation of sister chromatids occurs at meiosis II in sporulation deficient *cdc14* mutants

While looking at late time points in *cdc14*^{3HA} meiotic cells we observed a high frequency of cells with more than four nuclei (S1B and S3C Figs). This might be due to impediments during chromosome segregation in the first and/or the second division. To test this possibility, we analyzed the nuclear morphology, along with the meiotic spindle, in individual cells undergoing the first and second meiotic division (Fig 4A). Cells presenting MI spindle with a length of ≥5μm were considered to be in late anaphase I, and therefore, two DAPI masses should be distinguishable. On the other hand, those cells presenting DAPI bridges at the end of anaphase I might reflect those cells with some form of chromosome entanglement [45].

Wild-type cells showed clear separation of nuclear content in 74% of anaphases analyzed, and only ~25% of anaphases I presented DAPI bridges (Fig 4A). By contrast, *cdc14* cells had only ~20% of fully resolved two nuclei after anaphase I. Over 80% of *cdc14*^{3HA} mutant anaphases presented some kind of chromosomal bridges, suggesting that despite cells having undergone MI spindle elongation correctly, some form of DNA entwining was not properly resolved.

Chromosomal bridges observed in the mutant and the wild type at the end of anaphase I could be due to transitory entanglement of lagging, under-condensed chromosomal domains, that could be eventually resolved before the initiation of the second meiotic division. To test whether these bridges were eventually eliminated or instead, they remained as chromosomal intertwined; we looked at metaphase II cells and scored the configuration of their nuclear masses (Fig 4A, bottom panels). The wild type presented over 76% of metaphase II cells with single individualized nuclei located within each MII spindle whereas only 25% of *cdc14*^{3HA} mutant metaphase II cells displayed this configuration. In contrast, 75% of metaphase II cells in the *cdc14*^{3HA} mutant showed DNA threads connecting both nuclear masses. We can conclude that diminished levels of Cdc14 in meiosis enhances the formation of nuclear bridges after the first meiotic division and these bridges persist at least until metaphase II.

To determine whether these DAPI bridges present at metaphase II mutant cells are the consequence or the cause of other problems arising during chromosome segregation, we constructed strains carrying fluorescent markers on specific chromosomes and followed their segregation [71]. We made use of *tetO* repeats integrated at the interstitial *lys2* locus of chromosome II, together with the presence of the *tetR* repressor gene fused with GFP, which associates to these repeats [72]. A second strain with a different GFP reporter was made, but in this case, it carried *lacO* repeats in a centromere-proximal region at the *trp1* locus of chromosome IV, with a *lacI* repressor gene fused to GFP integrated at the *ura3* locus [73]. First, we analyzed strains carrying *LYS2-GFP* on both homologs to determine chromosome segregation fidelity in cells that had completed both meiotic divisions. In this way, we were able to visualize four individual dots segregating to each of the four nuclei within a single tetranucleated cell. The results showed chromosome II segregated correctly in 92% of wild-type cells. Remarkably, only 42% of *cdc14*^{3HA} tetranucleated cells presented the correct GFP distribution, whereas the remaining 58% of mutant cells displayed, at least, one of the four nuclei lacking a GFP focus (Fig 4B; S4 Fig). To understand the origin of the high levels of chromosome missegregation in the *cdc14*^{3HA}

cells we further analyzed the first and the second division separately. In order to determine correct homolog disjunction, we first analyzed binucleated cells using strains carrying the *CENIV-GFP* tag in homozygosity. We found that *cdc14*^{3HA} mutation did not enhance missegregation of homologs during the first meiotic division (Fig 4C). Very similar results were previously reported for homozygous *CENV-GFP* in *cdc14-1* mutants [53]. Next, we analyzed for correct sister chromatid segregation in the second meiotic division. Thus, heterozygous strains for the *CENIV-GFP* marker were used; 89% of wild-type cells showed correct sister separation after meiosis II. In contrast, 40% of *cdc14*^{3HA} cells displayed problems segregating sister centromeres (Fig 4D). Taken all together, we conclude that accurate sister chromatid segregation in meiosis requires unperturbed Cdc14 activity.

Meiotic recombination enhances the sporulation defect in *cdc14*^{3HA}

We considered that the increase in sister chromatid missegregation after the second division in *cdc14*^{3HA} cells, could be in part originated by aberrant recombination causing entanglements between sister chromatids. If that would be the case, we should be able to alleviate some of the sporulation problems associated to the *cdc14*^{3HA} mutation by eliminating meiotic recombination. To test this hypothesis we combined the *cdc14*^{3HA} allele with the *spo11* mutation, which prevents DSB formation [1]. The absence of DSBs partly restored sporulation in the *cdc14*^{3HA} mutant (Fig 4E); therefore, recombination enhances the sporulation defect observed in *cdc14*^{3HA} strains. Next, we thought that problems occurring at post-MI stages in meiosis could be the main causative factor of the sporulation defect in the *cdc14*^{3HA} mutant. Thus, eliminating a second round of chromosomal division might restore sporulation. To test this, we generated double mutants of *cdc14*^{3HA} and *spo13Δ*. Cells carrying *spo13Δ* display a single meiotic division due to premature sister chromatid separation and sister kinetochore bi-orientation at meiosis I, thus, *spo13Δ* cells preferentially form dyads with two diploid spores instead of tetrads [73-76]. As previously described, *spo13Δ* generated mostly dyads, with a sporulation efficiency of 78% after 72 hours following meiotic induction. Interestingly, *spo13Δ* mutation rescued the *cdc14*^{3HA} sporulation block allowing the double mutant to form spores to a frequency higher than 40% of total cells (Fig 4E). This is a notable rescue given that *cdc14*^{3HA} sporulation efficiency normally stays below 10-15%. Furthermore, the restoration of sporogenic potential for *cdc14*^{3HA} observed in the presence of *spo13Δ* mutation is accompanied by an increase in the formation of monads instead of dyads. Thus, we conclude that *spo13Δ* mutation greatly rescues the *cdc14*^{3HA} sporulation defect phenotype by skipping a second meiotic division but not by eliminating the non-disjunction problem.

Meiotic recombination is impaired in *cdc14*^{3HA} mutants

Elimination of Spo11-dependent DSBs robustly alleviates problems with chromosome segregation in FEAR mutants or in a *cdc14-1* background [45]. We have also shown that the sporulation defects can be partly rescued by eliminating recombination in *cdc14*^{3HA} mutants (Fig 4E). Thus, it seems that Cdc14

plays a fundamental role in promoting accurate repair of Spo11-dependent DSBs. To get more insights in the function of Cdc14 during meiotic recombination, we analyzed the well-studied *HIS4-LEU2* meiotic hotspot (Fig 5A-B; [77-80]) in the presence and absence of the *cdc14*^{3HA} mutation. First, we analyzed total levels of CO products; unexpectedly, total CO levels were subtly increased in the mutant in comparison with wild-type levels (Fig 5C). We also noticed a two-fold enrichment in the levels of higher molecular weight meiosis-specific bands, corresponding to ectopic recombination products with the endogenous Chr III *leu2* locus [81] (Fig 5B-C). Thus, Cdc14 normal activity is required to restrain ectopic recombination in meiotic cells. Next, we wondered how the higher levels of ectopic recombination and additional COs were first originated in the mutant. For that, we examined earlier recombination intermediates by 2D-gel analysis using the same hotspot (Fig 5A,D). Different DNA species were quantified at different times from synchronous meiotic cultures. We started visualizing dHJs intermediates from 4 hours until ~7-8.5 hours in both the wild type and the mutant (Fig 5E-F). Levels of dHJs were similar in both wild-type and *cdc14*^{3HA} strains (Fig 5E-G). Remarkably, we detected at 5 and 6 hours predominantly, the accumulation of higher levels of complex branched joint molecules (mc-JMs) in *cdc14*^{3HA}, which were not observed at any time in the wild type (Fig 5E-G). Levels of mc-JMs decreased slightly before the time dHJs were resolved, thus most of the accumulation of those complex JMs are finally processed. Therefore, the presence of multi-chromatid recombination intermediates together with the increase in ectopic recombinants (Fig 5C) are normally prevented by the action of the Cdc14 phosphatase. Thus, chromosome missegregation observed in *FEAR* and *cdc14-1* mutants [44,45] as well as for sister chromatids in *cdc14*^{3HA} mutants, are likely caused by abnormal accumulation, and processing, of Spo11-dependent JMs in the absence of Cdc14 activity.

Presence of toxic recombination species causes a delay in prophase I without activating the Meiotic Recombination Surveillance (MRS) network.

Next, we wondered whether the presence of higher frequency of an atypically abundant population of mc-JMs could trigger some form of checkpoint response or delay in prophase I. To test this possibility, we first studied the kinetics of synaptonemal complex (SC) assembly and disassembly by live cell imaging, as a readout of pachytene arrest. A GFP-tagged version of the central element component of the SC, Zip1 [82] was used. In brief, control and mutant cells were synchronized in parallel into meiosis and after 3 hours in SPM, images were then acquired for every 10 minutes up to 12 hours (Fig 6A). Nuclei displaying maximum GFP intensity were quantified for each timepoint and frequencies among the total population plotted over time. Thus, control Zip1-GFP positive cells reached a maximum at 300-320 minutes into the timecourse. Finally, the number of nuclei presenting Zip1-GFP signal decayed to almost background levels by eight hours, becoming undetectable by the end of the time-course (Fig 6B). *cdc14*^{3HA} cells acquired nuclei with Zip1-GFP positive signal at similar kinetics as wild-type cells. Noteworthy, *cdc14*^{3HA} mutant cells reached a maximum of nuclei in pachynema by around 340-360

minutes post-meiotic induction, but quickly dropped to initial Zip-GFP signal basal levels very close the wild-type kinetics (Fig 6B). Nonetheless, the extended period in pachytene-like stage was accompanied by an increase in the total number of cells with respect to the wild type (S5 Fig), suggesting that the delay was in fact a transitory accumulation of cells in such stage.

We next examined whether the delay observed in *cdc14*^{3HA} cells at pachynema was monitored by the meiotic recombination surveillance network, active during prophase I [83-85]. Western blot analysis using anti-phosphorylated Threonine 318 in Hop1, a *bona-fide* marker of meiosis specific Mec1/ATR kinase activity, and recombination checkpoint, displayed no observable difference in between the control, and mutant backgrounds (Fig 6C). This suggests that the delay observed in *cdc14*^{3HA} mutant in pachynema might not trigger a robust checkpoint response.

Yen1 helps resolve aberrant recombination intermediates originated in the absence of Cdc14

The requirement of Cdc14 for the correct repair of Spo11-dependent DSBs, led us to search for suitable candidates that could be regulated by the phosphatase in meiosis. Yen1 has been nominated as a target of Cdc14 in mitotic cells in the presence of DNA damage [18,19,86]. Thus, to study whether Yen1 could be a target of Cdc14 during meiosis, we tested the activity of the nuclease during a meiotic time course in the presence, or absence, of *cdc14*^{3HA} mutant. Thus, samples were collected every two hours from synchronized meiotic cultures of wild-type and *cdc14*^{3HA} cells, each of them carrying a functional tagged version of the *YEN1* gene fused to 9 copies of the *MYC* epitope [17]. From each time-point, Yen1-9Myc was immunoprecipitated from the meiotic extracts and beads carrying the protein were incubated with a synthetic Holliday Junction substrate [87]. Active nuclease should be able to cut the HJ substrate whereas the phosphorylated inactive form of the enzyme would not. In wild-type diploid cells, Yen1-9myc did not display any nuclease activity during early stages of the meiotic time course. In SK1 synchronous meiotic cultures, S-phase and prophase I takes usually about six hours to be completed. The estimated length of pre-MI stages was also confirmed by the absence of Cdc5 in the lanes corresponding to those hours (Fig 6D). Very little activity for Yen1 was detected during that period except for the residual endonuclease activity observed at t=0 hours, which might reflect the activity of a small sub-population of asynchronous cells still undergoing mitotic divisions. The maximum activity observed for Yen1 in wild-type meiotic cells corresponded from t=10 to t=12 hours after induction of meiosis, which usually corresponds to cells in meiosis II (Fig 6D, F; [15]). Notably, the resolvase activity displayed by Yen1 in *cdc14*^{3HA} cultures was low during the entire length of the time course (Fig 6D, F). We considered that *cdc14* mutant cells were transiting at similar kinetics as wild-type cells through the time course given that meiotic S-phase was completed on similar timing for both strains (Fig 6E). Moreover, detectable levels of Cdc5 protein corresponded with the same hours as

the wild-type culture. These data strongly suggest that Cdc14 is required for Yen1 activation during meiosis II.

Next, we sought to eliminate the requirement of Cdc14 phosphatase for Yen1 activation by directly using a phospho-resistant version of the nuclease (*YEN1*^{ON}). Elimination of nine of the CDK consensus sites of phosphorylation in Yen1 renders the protein constitutively active [17,19]. We combined *cdc14*^{3HA} allele with *YEN1*^{ON} and tested for sporulation efficiency. Similar to the elimination of Spo11 DSBs, unrestrained activity of Yen1 restored in part the sporulation defect of *cdc14*^{3HA} (Fig 6G), confirming that Yen1 activation by Cdc14 is important for late resolution of toxic recombination intermediates.

Discussion

Meiotic recombination is fundamental for sexual reproduction, ensuring that homologous chromosomes segregate correctly at the first meiotic division as well as to facilitate distinct allele combinations that sustain evolution. Homologous recombination is initiated by the introduction of programmed DSBs ensued by homologue pairing and DNA strand exchange. Those early steps in the recombination process lead to the formation of stable JMs, which are ultimately resolved into two main classes of HR repair products, known as COs and NCOs (Fig 7). Recombining chromosomes may also contain intermediates consisting of three- and four-armed DNA structures such as mc-JMs, where three and four DNA duplexes stay connected (Fig 7; [8,9,79,88-92]). In some cases, unresolved recombination intermediates might persist until the metaphase to anaphase transition where a subset of late-acting nucleases process them in order to safeguard genome integrity. Unrestrained activity of such nucleases can interfere with the correct allotment of COs and NCOs in meiosis [17], thus, they are tightly controlled by several layers of regulation. Posttranslational modifications carried out principally by key cell cycle kinases, like CDK, DDK, and PLK1, are the most extended form of regulation [15]. Additionally, at least one of the late acting nucleases, Yen1, has been described as modulated through the highly conserved Cdc14 phosphatase in mitotic cells [18,19,86]. Given the essentiality of *CDC14* in *S. cerevisiae*, most meiotic studies performed to date have required the use of conditional temperature sensitive alleles of *cdc14* that cannot complete meiosis following the first round of chromosome segregation [21,45,55,66]. Despite the large amount of valuable data that has been collected over the past years using these alleles, other less conspicuous functionalities of Cdc14, particularly those affecting meiosis II, might have been precluded from being discovered when studying meiosis in *cdc14 ts* mutants. Here, using a different meiotic-deficient allele of *CDC14* we have been able to identify previously undetected functions of the phosphatase during meiosis, particularly those affecting the second meiotic division (Fig 7). Furthermore, we found the unprecedented requirement of *CDC14* to prevent the accumulation of mc-JMs during meiotic prophase I, suggesting that Cdc14 regulates other

not yet identified enzymatic activities that are required for the early resolution of these branched molecules.

Novel insights into Cdc14 functionalities by using an epitope-tagged version of the phosphatase

In the present study we describe an allele of *CDC14* (*cdc14^{3HA}*) that displays no obvious defects during unchallenged mitotic divisions; nonetheless, it is strongly deficient in sporulation during meiosis. *cdc14^{3HA}* is a C-terminal tagged version of *CDC14* with three copies of hemagglutinin, which has been used in other studies to monitor its behaviour during mitosis [23,32,35] and in meiosis [49]. Protein levels of the phosphatase are severely reduced in homozygous *cdc14^{3HA}* meiotic cells (Fig 2A-B), a problem not perceived during the mitotic cell cycle, when 3xHA is fused at the N-terminal end of Cdc14 [45], or when *cdc14^{3HA}* is present in heterozygosity together with the wild-type *CDC14* gene [93]. *cdc14^{3HA}* mutant cells complete meiotic DNA replication and both nuclear divisions with kinetics not too dissimilar from those of the wild type, suggesting that both rounds of chromosome segregation take place in *cdc14* meiotic cells. Nonetheless, the *cdc14^{3HA}* mutant failed to form spores once cells completed both nuclear divisions. We exclude that the process of spore formation was affected since we visualized pro-spore membrane components appearing at similar kinetics in the mutant strain as they did in the wild type (S5 Fig). Other groups have also described similar defects in sporulation in the absence of Cdc14 activity, or components of the MEN pathway [48,94]. The fact that we monitored correct SPB re-duplication and separation in a high proportion of *cdc14^{3HA}* cells (Fig 2C-D; S3 Fig), and that they are able to assemble functional spindles at metaphase/anaphase II also confirms that problems arising in *cdc14^{3HA}* mutant somewhat differ from those already described for the widely employed, thermo-sensitive alleles, *cdc14-1, -3* or other FEAR mutants [45,53,55]. One possibility is that differences in the mechanism by which Cdc14 activity is depleted during meiosis might be accountable for the observed variations in the meiotic behaviour. Even so, most of the described phenotypical features regarding the recombination-dependent missegregation are conserved for *cdc14^{3HA}* (Fig 4), so our allele recapitulates those impaired functionalities linked to the recombination defect previously observed. Notwithstanding, meiotic divisions occur in most *cdc14^{3HA}* cells, with no discernible delay in spindle dynamics when compared to wild-type cells (Fig 3B-C). A very subtle delay, observed during both divisions, could in part arise from difficulties in SPB re-duplication and half-bridge separation, as described in *cdc14-1* cells [55]. Similarly, inactivation of Cdc14 in cells transiting metaphase II, did not show any effect on the lifetime of meiosis II spindles [94], confirming that the phenotype we observe can be reproduced under different modes of *cdc14* inactivation during meiosis. Moreover, the meiotic delays observed in *cdc14^{3HA}* are not restricted to the completion of meiotic divisions. Surprisingly, delays are also detected when exiting the pachytene stage at prophase I (Fig 6B). Interestingly, phosphorylation of Hop1-T318 is not induced in *cdc14^{3HA}* cells suggesting that the insult that causes the pachytene delay is of transitory nature, and it is not fully sensed by the meiotic

checkpoint machinery (Fig 6C). The extended pachytene stage observed in *cdc14*^{3HA} cells is paralleled by the accumulation of complex branched recombination intermediates and the appearance of ectopic recombination products. Strikingly, levels of sister chromatids missegregation, but not of homologs, are substantial once *cdc14*^{3HA} cells endured the second meiotic division, suggesting that formation of ectopic recombinant products during prophase I could affect sister chromatid disjunction more acutely than that of homologs. These results again highlight the importance of safeguarding correct genome repair during the entire length of the meiotic cell cycle. Non-disjunction at either first or second division could likewise bring severe consequences to the correct ploidy of the developing gametes.

CDC14-dependent resolution of complex recombination intermediates via multiple mechanisms

The appearance of mc-JMs should occur alongside with other JMs, around pachytene, far earlier than the first release of Cdc14 at anaphase I has been reported during meiosis. Nevertheless, this is not the first time that the requirement of Cdc14 has been linked to cell cycle stages that precedes its bulk release from the nucleolus. Cdc14 has been involved in completion of late-replicating regions in the rDNA, and other parts of the genome. Such problems arise due to dosage insufficiency of replication factors, although those deficiencies, in principle, seemed to be contingent on the reduced Cdc14 activity in preceding mitoses in the *cdc14-1* allele used for such study [41]. Notwithstanding, collision amidst transcription and replication due to absence of Cdc14-mediated transcriptional silencing during S-phase is expected to hamper the completion of DNA replication. Irrespectively, the insufficient dosage of replication factors in *cdc14* cells stemmed from two main reasons: i) nuclear import is constitutively impaired in *cdc14* cells, preventing essential replication factors to properly enter the nucleus. Such is the case for certain subunits of RPA, and ii) reduced transcription of genes controlled by MBF and SBF transcription complexes in G1 which translates into reduced protein levels. The accumulation of aberrant recombination intermediates observed at the *HIS4-LEU2* hotspot in *cdc14*^{3HA} mutant might as well be consequence of the reduced activity of the Cdc14^{3HA} phosphatase during previous pre-meiotic mitotic divisions. Furthermore, Swi6, a transcription factor member of MBF and SCF complexes, requires of the de-phosphorylation of its phospho-Serine 160 by Cdc14, in order to be imported to the nucleus upon mitotic exit [95]. Swi6 has been also shown to be important in meiotic cells [96] and the expression of genes like *RAD54* and *RAD51* is downregulated in a *swi6* mutant. Furthermore, intragenic recombination frequencies between *his4-4* and *his4-290* was decreased considerably in the *swi6* mutant, suggesting that the earlier accumulation of mc-JMs might be consequence of a reduced dosage of recombination genes. Puzzlingly, we observed higher frequency of COs and ectopic recombination products at the *HIS4-LEU2* hotspot in the *cdc14*^{3HA} mutant compared to control cells, in the same way as we observed similar frequencies of IH-dHJ in our 2D gel studies for wild-type and *cdc14* cells. Such observations would argue against reduced dosage of recombination genes in *cdc14*^{3HA} mutants during

meiosis. On the other hand, it is also possible that only a subset of those recombination genes, important for preventing the accumulation of mc-JMs, is affected by Swi6 nuclear depletion in *cdc14* mutants, although such effect of Cdc14^{3HA} over Swi6 would need to be tested first in meiotic cells. In contrast, we favour a role of Cdc14 by directly regulating substrates required for averting mc-JM accumulation [4,10,15]. Interestingly, the conserved SSE, Yen1^{GEN1} is a critical substrate of Cdc14 during budding yeast's mitosis, and it exhibits nucleocytoplasmic shuttling using a similar phospho-regulatory behaviour as that of Swi6 [97]. Namely, CDK-dependent phosphorylation restricts Yen1 from entering the nucleus and becoming active, whereas reversal of that phosphorylation by Cdc14 allows Yen1 to enter the nucleus and resolve those DNA-structures [18,19,86]. Nonetheless, Yen1 nuclear import and activation appears to be concomitant with bulk Cdc14 release from the nucleolus during anaphase. This is why a role for Yen1 in safeguarding chromosome segregation has been proposed, especially at meiosis II. Our results support such conclusion, since higher frequencies of aneuploidies and missegregation are detected during meiosis II for a *cdc14^{3HA}* meiotic mutant (Fig 4D), consistent with the expected ability of Cdc14 to activate Yen1 (Fig 6D). Whether or not Yen1 acts during anaphase I is still unclear. Nuclear localization of Yen1 is moderately high at anaphase I and maximum during anaphase II, but its endonucleolytic activity only turns pervasive concomitant with the appearance of MII spindles ([17]; Fig 6D). Perhaps, minimal nuclear localization does not necessarily boost Yen1 activity, which might require additional regulatory modifications only present at the second stage of meiotic divisions. Interestingly, it has been shown that Cdc14 gets only fully released to the cytoplasm during the second meiotic division, whereas the first division confines Cdc14 diffusion within just the nucleoplasm [46]. Unrestrained action of Yen1, by means of a phospho-depleted allele of the endonuclease, *YEN1^{ON}*, partly restores sporulation in *cdc14^{3HA}* diploid cells, suggesting that lack of Yen1 activity is somewhat responsible of the severity of the *cdc14^{3HA}* meiotic phenotype, but not entirely (Fig 6G).

Additional meiosis-specific substrates of Cdc14 during gametogenesis.

It has been known for some time that *cdc14* and FEAR mutants display problems segregating chromosomes in a *SPO11*-dependent way [44,45]. Similarly, the *cdc14^{3HA}* sporulation defect was somewhat solved when eliminating Spo11 activity (Fig 4E).

Recombination at the rDNA does not occur during meiotic prophase I [98], a process actively inhibited due to the exclusion of Hop1 from the nucleolus [99-101] thus, difficulties segregating this region do not seem to be the origin of the *SPO11*-dependent entanglements. Nonetheless, although unlikely, an inhibitory role of Cdc14 in *SPO11*-mediated recombination at the rDNA has not been tested yet, to our knowledge. On the other hand, a number of DNA-repair proteins present at the nucleolus early in prophase I might require of Cdc14 activity *in situ* in order for these enzymes, or their activities, to spread outside the rDNA. Such role of Cdc14 directly from the nucleolus would aid resolving complex

mc-JMs generated as part of homologous recombination repair endeavours, without compromising the allotment of enzymes essential for correct rDNA functionality.

An alternative interpretation may well be made if multiple nuclear substrates required for JM resolution would participate, either during the transition from the pachytene stage to metaphase I or during anaphase I, upon bulk release of the phosphatase from the nucleolus. The first scenario would suit better with the timing of resolution of mc-JM in our studies, and it might require early release of Cdc14, or a subpopulation of the phosphatase, a possibility that, to our knowledge, has not been reported yet for meiotic cells. Strikingly, DNA damage caused in vegetative cells triggers the transitory release of Cdc14 to the nucleoplasm from the nucleolus, allowing the phosphatase to act over components of the SPBs and to stabilize them at metaphase [42]. Additionally, sub-populations of Cdc14 have been observed at different subcellular structures during mitosis and meiosis, including kinetochores, bud neck and SPBs/centrosomes [55,102,103]. In budding yeast meiosis, the timing of JM resolution and CO formation is coordinated with cell-cycle progression through the *NDT80*-dependent expression of the Polo-like kinase Cdc5 [13-15]. Thus, unlike mitotic cells, an earlier requirement of Cdc5 for the resolution of dHJ at the pachytene to MI transition, upon Ndt80 activation, might too impinge on its ability to interact with Cdc14 and Cif1/Net1 in the nucleolus. Such interaction might counteract temporally the negative regulatory effect of $PP2A^{Cdc55}$ allowing some Cdc14 molecules to escape from its captor [42,52,53]. We are tempted to speculate that Cdc5 might play a relevant role during meiosis in promoting the early-release of a population of Cdc14 at the transition from pachynema to anaphase I in order to modulate the activity of a number of safeguarding enzymes required for correct chromosome segregation. Further studies will be required to determine whether that last possibility is true, or if other regulators, like those involved in the DDR, are also involved.

In recent years, human orthologues of Cdc14 phosphatase have received increased attention due to their involvement in key processes like DDR, DNA repair and cell cycle control. Furthermore, recent findings point to recessive variants of the phosphatase to be directly responsible of human diseases, like deafness and male infertility [104]. Thus, in order to comprehend the underlying factors that trigger those conditions, it will require a deeper understanding of the genetic and molecular mechanisms that are responsible of the countless functionalities, and targets yet to be identified, of the Cdc14 phosphatase during gametogenesis and HR repair.

Materials and Methods

All strains were SK1, as detailed in S1 Table. Standard yeast manipulation procedures and growth media are utilized. To introduce the (3HA) tag at the C-terminal end of Cdc14, the CDC14ha3-$pKan^R$ plasmid containing the last ~500bps of the *CDC14* gene, cloned in frame with 3xHA using the NotI restriction site, and containing the *CLB1* terminator. The plasmid was linearized using a unique restriction site located within the *CDC14* sequence and the linearized plasmid was transformed into a SK1 haploid strain. Alternatively, *CDC14* was tagged using the PCR-based method described in [105] using the

plasmid pFA6a-ha3-kanMX6. The phenotype of *CDC14-3HA* strains obtained from both tagging methods were checked and the sporulation defect was identical. Transformants containing correct tag integration were identified and tested by western blot for the presence of the tag, Southern blot analysis and/or PCR was performed to confirm the integration at the endogenous locus.

Synchronous meiotic time course

Induction of synchronous meiosis is carried out according to the established protocols for standard assays [106]. All pre-growth and meiotic time courses were carried out at 30°C unless specified otherwise. For *cdc14-1* meiosis, the culture was kept at 23°C and shifted to 30°C 2 hours after transferring into sporulation medium (SPM). An aliquot was removed at the specified time, and subjected to various analyses.

DNA manipulation, extraction and southern blot detection

Standard DNA extraction was performed as in [107]. For studies at the *HIS4-LEU2* recombination hotspot, the protocol described in [108] was followed. For 2D gel agarose electrophoresis, cell cultures were psoralen photo-crosslinked with longwave UV light before DNA extraction, in order to visualize recombination intermediates by standard southern blotting techniques at the *HIS4-LEU2* hotspot [108]

Time-lapse imaging, microscopy, and image analysis

Time-lapse experiments were performed as in [109], with small variations. In brief, 1 ml aliquots from synchronous meiotic cultures were taken at specific times, diluted 1:9 in fresh SPM (kept at 30°C). 300µl of diluted cells were placed in suitable multi-well slides 80821 uncoated, ibidi). Slides were placed in a temperature controlled incubation chamber from a Multidimensional Microscopy System Leica AF6000 LX. Images were taken at multiple positions and channels every 5, 10 or 15 minutes, depending on the experiment. Image acquisition was carried out using a CCD Hamamatsu 9100-02 camera. The system was controlled by the proprietary software, Leica Application Suite X, version 3.30. For preparations of fixed cells, aliquots were fixed and prepared as described in [107]. Chromosomal DNA was stained with 1µg/ml 4,6-diamino-2-phenylimide (DAPI). Images were recorded and analyzed using a Deltavision (DV3) workstation from Applied Precision Inc. with a Photometrics CoolSnap HQ (10-20MHz) air cooled CCD camera and controlled by Softworx image acquisition and deconvolution software.

Protein extraction, Western blot analysis and antibodies

Whole-cell extracts were prepared from cell suspensions in 20% trichloroacetic acid by agitation with glass beads. Precipitated proteins were solubilized in SDS-PAGE sample buffer, and appropriate dilutions were analyzed by SDS-PAGE and Western blotting. Antibodies for Western blotting were mouse monoclonal anti-MYC (1:1000, AbCam), mouse monoclonal anti-HA (1:1000) from S. Ley

(NIMR), rabbit polyclonal anti-Ssp1 (1:100), rabbit anti-Phospho-T318-Hop1 (1:1000), Cambridge Research Biomedicals), goat anti-mouse IgG conjugated to horseradish peroxidase (1:10000; Sigma-Aldrich), and chicken anti-rabbit IgG conjugated to horseradish peroxidase (1:10000; Sigma-Aldrich).

Nuclease assays

For nuclease assays, myc9-tagged Yen1 was immuno-affinity purified from yeast using anti-Myc agarose beads (9E10) and washed extensively. The beads (approx. volume 10 µl) were then mixed with 10 µl cleavage buffer (50 mM Tris-HCl pH 7.5, 3 mM $MgCl_2$) and 15 ng of 5'-Cy3-end-labeled synthetic Holliday junction X0 DNA. After 1 h incubation at 37°C with gentle rotation, reactions were stopped by addition of 2.5 µl of 10 mg/ml proteinase K and 2% SDS, followed by incubation for 30 min at 37°C. Loading buffer (3 µl) was then added and fluorescently-labelled products were separated by 10% native PAGE and analyzed using a Typhoon scanner and ImageQuant software. Resolution activity was calculated by determining the fraction of nicked duplex DNA product relative to the sum of the intact substrate and resolution product. The protein input was estimated by western blot.

Data analysis and Biostatistics

Data was compiled and analyzed using Excel, LibreOffice Calc, and SPSS Statistical Data Editor. For multiple comparisons, analysis of variance (one-way ANOVA) was performed. For pairwise comparisons, two-tailed unpaired t tests were used using IBM SPSS Statistics and SigmaPlot.

Acknowledgements

We would like to thank C.R. Vázquez de Aldana, M. Knop, E. Winter, A.M. Neiman, E. Hoffmann, J.L. Santos, G.V. Börner, A. Marston, M.G. Blanco and F. Machín for kindly providing us with reagents, strains, antibodies and/or advice. We are especially thankful to the Molecular Biology of the Chromosome lab for sharing lab space, reagents and equipment. We would like to thank to the microscopy facility at the CIB and to J.S. Ahuja, for valuable technical advice in designing and analysing time-lapse or 2D gel experiments, respectively.

References

1. Keeney S, Giroux CN, Kleckner N (1997) Meiosis-specific DNA double-strand breaks are catalyzed by Spo11, a member of a widely conserved protein family. Cell 88: 375-384.

2. Bishop DK (2006) Multiple mechanisms of meiotic recombination. Cell 127: 1095-1097.

3. Zakharyevich K, Ma Y, Tang S, Hwang PY, Boiteux S, et al. (2010) Temporally and biochemically distinct activities of Exo1 during meiosis: double-strand break resection and resolution of double Holliday junctions. Mol Cell 40: 1001-1015.

4. Zakharyevich K, Tang S, Ma Y, Hunter N (2012) Delineation of joint molecule resolution pathways in meiosis identifies a crossover-specific resolvase. Cell 149: 334-347.

5. de los Santos T, Loidl J, Larkin B, Hollingsworth NM (2001) A role for *MMS4* in the processing of recombination intermediates during meiosis in *Saccharomyces cerevisiae*. Genetics 159: 1511-1525.

6. Oh SD, Lao JP, Hwang PY, Taylor AF, Smith GR, et al. (2007) BLM ortholog, Sgs1, prevents aberrant crossing-over by suppressing formation of multichromatid joint molecules. Cell 130: 259-272.

7. Piazza A, Wright WD, Heyer WD (2017) Multi-invasions Are Recombination Byproducts that Induce Chromosomal Rearrangements. Cell 170: 760-773 e715.

8. Oh SD, Lao JP, Taylor AF, Smith GR, Hunter N (2008) RecQ helicase, Sgs1, and XPF family endonuclease, Mus81-Mms4, resolve aberrant joint molecules during meiotic recombination. Mol Cell 31: 324-336.

9. Jessop L, Lichten M (2008) Mus81/Mms4 endonuclease and Sgs1 helicase collaborate to ensure proper recombination intermediate metabolism during meiosis. Mol Cell 31: 313-323.

10. De Muyt A, Jessop L, Kolar E, Sourirajan A, Chen J, et al. (2012) BLM helicase ortholog Sgs1 is a central regulator of meiotic recombination intermediate metabolism. Mol Cell 46: 43-53.

11. Xaver M, Huang L, Chen D, Klein F (2013) Smc5/6-Mms21 prevents and eliminates inappropriate recombination intermediates in meiosis. PLoS Genet 9: e1004067.

12. Copsey A, Tang S, Jordan PW, Blitzblau HG, Newcombe S, et al. (2013) Smc5/6 coordinates formation and resolution of joint molecules with chromosome morphology to ensure meiotic divisions. PLoS Genet 9: e1004071.

13. Clyne RK, Katis VL, Jessop L, Benjamin KR, Herskowitz I, et al. (2003) Polo-like kinase Cdc5 promotes chiasmata formation and cosegregation of sister centromeres at meiosis I. Nat Cell Biol 5: 480-485.

14. Sourirajan A, Lichten M (2008) Polo-like kinase Cdc5 drives exit from pachytene during budding yeast meiosis. Genes Dev 22: 2627-2632.

15. Matos J, Blanco MG, Maslen S, Skehel JM, West SC (2011) Regulatory control of the resolution of DNA recombination intermediates during meiosis and mitosis. Cell 147: 158-172.

16. Ip SCY, Rass U, Blanco MG, Flynn HR, Skehel JM, et al. (2008) Identification of Holliday junction resolvases from humans and yeast. Nature 456: 357-361.

17. Arter M, Hurtado-Nieves V, Oke A, Zhuge T, Wettstein R, et al. (2018) Regulated Crossing-Over Requires Inactivation of Yen1/GEN1 Resolvase during Meiotic Prophase I. Dev Cell 45: 785-800.e786.

18. Eissler CL, Mazon G, Powers BL, Savinov SN, Symington LS, et al. (2014) The Cdk/cDc14 module controls activation of the Yen1 holliday junction resolvase to promote genome stability. Mol Cell 54: 80-93.

19. Blanco MG, Matos J, West SC (2014) Dual control of Yen1 nuclease activity and cellular localization by Cdk and Cdc14 prevents genome instability. Mol Cell 54: 94-106.

20. Visintin R, Craig K, Hwang ES, Prinz S, Tyers M, et al. (1998) The phosphatase Cdc14 triggers mitotic exit by reversal of Cdk-dependent phosphorylation. Mol Cell 2: 709-718.

21. Culotti J, Hartwell LH (1971) Genetic control of the cell division cycle in yeast. 3. Seven genes controlling nuclear division. Exp Cell Res 67: 389-401.

22. Hartwell LH, Mortimer RK, Culotti J, Culotti M (1973) GENETIC CONTROL OF THE CELL DIVISION CYCLE IN YEAST: V. GENETIC ANALYSIS OF *cdc* MUTANTS. Genetics 74: 267-286.

23. Shou W, Seol JH, Shevchenko A, Baskerville C, Moazed D, et al. (1999) Exit from mitosis is triggered by Tem1-dependent release of the protein phosphatase Cdc14 from nucleolar RENT complex. Cell 97: 233-244.

24. Visintin R, Hwang ES, Amon A (1999) Cfi1 prevents premature exit from mitosis by anchoring Cdc14 phosphatase in the nucleolus. Nature 398: 818-823.

25. Machín F, Torres-Rosell J, De Piccoli G, Carballo JA, Cha RS, et al. (2006) Transcription of ribosomal genes can cause nondisjunction. J Cell Biol 173: 893-903.

26. Clemente-Blanco A, Mayan-Santos M, Schneider DA, Machin F, Jarmuz A, et al. (2009) Cdc14 inhibits transcription by RNA polymerase I during anaphase. Nature 458: 219-222.

27. Clemente-Blanco A, Sen N, Mayan-Santos M, Sacristan MP, Graham B, et al. (2011) Cdc14 phosphatase promotes segregation of telomeres through repression of RNA polymerase II transcription. Nat Cell Biol 13: 1450-1456.

28. Yoshida S, Toh-e A (2002) Budding yeast Cdc5 phosphorylates Net1 and assists Cdc14 release from the nucleolus. Biochem Biophys Res Commun 294: 687-691.

29. Visintin R, Stegmeier F, Amon A (2003) The role of the polo kinase Cdc5 in controlling Cdc14 localization. Mol Biol Cell 14: 4486-4498.

30. Azzam R, Chen SL, Shou W, Mah AS, Alexandru G, et al. (2004) Phosphorylation by cyclin B-Cdk underlies release of mitotic exit activator Cdc14 from the nucleolus. Science 305: 516-519.

31. Queralt E, Lehane C, Novak B, Uhlmann F (2006) Downregulation of PP2A(Cdc55) phosphatase by separase initiates mitotic exit in budding yeast. Cell 125: 719-732.

32. Rahal R, Amon A (2008) The Polo-like kinase Cdc5 interacts with FEAR network components and Cdc14. Cell Cycle 7: 3262-3272.

33. Rodriguez-Rodriguez JA, Moyano Y, Jativa S, Queralt E (2016) Mitotic Exit Function of Polo-like Kinase Cdc5 Is Dependent on Sequential Activation by Cdk1. Cell Rep 15: 2050-2062.

34. Stegmeier F, Visintin R, Amon A (2002) Separase, polo kinase, the kinetochore protein Slk19, and Spo12 function in a network that controls Cdc14 localization during early anaphase. Cell 108: 207-220.

35. Visintin C, Tomson BN, Rahal R, Paulson J, Cohen M, et al. (2008) APC/C-Cdh1-mediated degradation of the Polo kinase Cdc5 promotes the return of Cdc14 into the nucleolus. Genes Dev 22: 79-90.

36. Hartwell LH, Smith D (1985) Altered fidelity of mitotic chromosome transmission in cell cycle mutants of S. cerevisiae. Genetics 110: 381-395.

37. D'Amours D, Stegmeier F, Amon A (2004) Cdc14 and condensin control the dissolution of cohesin-independent chromosome linkages at repeated DNA. Cell 117: 455-469.

38. Sullivan M, Higuchi T, Katis VL, Uhlmann F (2004) Cdc14 phosphatase induces rDNA condensation and resolves cohesin-independent cohesion during budding yeast anaphase. Cell 117: 471-482.

39. Torres-Rosell J, Machin F, Jarmuz A, Aragon L (2004) Nucleolar segregation lags behind the rest of the genome and requires Cdc14p activation by the FEAR network. Cell Cycle 3: 496-502.

40. Wang BD, Yong-Gonzalez V, Strunnikov AV (2004) Cdc14p/FEAR pathway controls segregation of nucleolus in S. cerevisiae by facilitating condensin targeting to rDNA chromatin in anaphase. Cell Cycle 3: 960-967.

41. Dulev S, de Renty C, Mehta R, Minkov I, Schwob E, et al. (2009) Essential global role of *CDC14* in DNA synthesis revealed by chromosome underreplication unrecognized by checkpoints in *cdc14* mutants. Proc Natl Acad Sci U S A 106: 14466-14471.

42. Villoria MT, Ramos F, Duenas E, Faull P, Cutillas PR, et al. (2017) Stabilization of the metaphase spindle by Cdc14 is required for recombinational DNA repair. EMBO J 36: 79-101.

43. Sharon G, Simchen G (1990) Mixed segregation of chromosomes during single-division meiosis of *Saccharomyces cerevisiae*. Genetics 125: 475-485.

44. Buonomo SB, Rabitsch KP, Fuchs J, Gruber S, Sullivan M, et al. (2003) Division of the nucleolus and its release of *CDC14* during anaphase of meiosis I depends on separase, *SPO12*, and *SLK19*. Dev Cell 4: 727-739.

45. Marston AL, Lee BH, Amon A (2003) The Cdc14 phosphatase and the FEAR network control meiotic spindle disassembly and chromosome segregation. Dev Cell 4: 711-726.

46. Yellman CM, Roeder GS (2015) Cdc14 Early Anaphase Release, FEAR, Is Limited to the Nucleus and Dispensable for Efficient Mitotic Exit. PLoS One 10: e0128604.

47. Kamieniecki RJ, Liu L, Dawson DS (2005) FEAR but not MEN genes are required for exit from meiosis I. Cell Cycle 4: 1093-1098.

48. Pablo-Hernando ME, Arnaiz-Pita Y, Nakanishi H, Dawson D, del Rey F, et al. (2007) Cdc15 is required for spore morphogenesis independently of Cdc14 in *Saccharomyces cerevisiae*. Genetics 177: 281-293.

49. Attner MA, Amon A (2012) Control of the mitotic exit network during meiosis. Mol Biol Cell 23: 3122-3132.

50. Kamieniecki RJ, Shanks RM, Dawson DS (2000) Slk19p is necessary to prevent separation of sister chromatids in meiosis I. Curr Biol 10: 1182-1190.

51. Zeng X, Saunders WS (2000) The *Saccharomyces cerevisiae* centromere protein Slk19p is required for two successive divisions during meiosis. Genetics 155: 577-587.

52. Kerr GW, Sarkar S, Tibbles KL, Petronczki M, Millar JB, et al. (2011) Meiotic nuclear divisions in budding yeast require PP2A(Cdc55)-mediated antagonism of Net1 phosphorylation by Cdk. J Cell Biol 193: 1157-1166.

53. Bizzari F, Marston AL (2011) Cdc55 coordinates spindle assembly and chromosome disjunction during meiosis. J Cell Biol 193: 1213-1228.

54. Nolt JK, Rice LM, Gallo-Ebert C, Bisher ME, Nickels JT (2011) PP2A (Cdc)(5)(5) is required for multiple events during meiosis I. Cell Cycle 10: 1420-1434.

55. Fox C, Zou J, Rappsilber J, Marston AL (2017) Cdc14 phosphatase directs centrosome re-duplication at the meiosis I to meiosis II transition in budding yeast. Wellcome Open Res 2: 2.

56. Mocciaro A, Schiebel E (2010) Cdc14: a highly conserved family of phosphatases with non-conserved functions? J Cell Sci 123: 2867-2876.

57. Li L, Ernsting BR, Wishart MJ, Lohse DL, Dixon JE (1997) A family of putative tumor suppressors is structurally and functionally conserved in humans and yeast. J Biol Chem 272: 29403-29406.

58. Rosso L, Marques AC, Weier M, Lambert N, Lambot MA, et al. (2008) Birth and rapid subcellular adaptation of a hominoid-specific CDC14 protein. PLoS Biol 6: e140.

59. Trautmann S, McCollum D (2002) Cell cycle: new functions for Cdc14 family phosphatases. Curr Biol 12: R733-735.

60. Bassermann F, Frescas D, Guardavaccaro D, Busino L, Peschiaroli A, et al. (2008) The Cdc14B-Cdh1-Plk1 axis controls the G2 DNA-damage-response checkpoint. Cell 134: 256-267.

61. Mocciaro A, Berdougo E, Zeng K, Black E, Vagnarelli P, et al. (2010) Vertebrate cells genetically deficient for Cdc14A or Cdc14B retain DNA damage checkpoint proficiency but are impaired in DNA repair. J Cell Biol 189: 631-639.

62. Diaz-Cuervo H, Bueno A (2008) Cds1 controls the release of Cdc14-like phosphatase Flp1 from the nucleolus to drive full activation of the checkpoint response to replication stress in fission yeast. Mol Biol Cell 19: 2488-2499.

63. Briza P, Winkler G, Kalchhauser H, Breitenbach M (1986) Dityrosine is a prominent component of the yeast ascospore wall. A proof of its structure. J Biol Chem 261: 4288-4294.

64. Bloom J, Cross FR (2007) Novel role for Cdc14 sequestration: Cdc14 dephosphorylates factors that promote DNA replication. Mol Cell Biol 27: 842-853.

65. Zickler D, Kleckner N (2015) Recombination, Pairing, and Synapsis of Homologs during Meiosis. Cold Spring Harb Perspect Biol 7.

66. Schild D, Byers B (1980) Diploid spore formation and other meiotic effects of two cell-division-cycle mutations of *Saccharomyces cerevisiae*. Genetics 96: 859-876.

67. Avena JS, Burns S, Yu Z, Ebmeier CC, Old WM, et al. (2014) Licensing of yeast centrosome duplication requires phosphoregulation of *sfi1*. PLoS Genet 10: e1004666.

68. Moens PB, Rapport E (1971) Spindles, spindle plaques, and meiosis in the yeast *Saccharomyces cerevisiae* (Hansen). J Cell Biol 50: 344-361.

69. Neiman AM (1998) Prospore membrane formation defines a developmentally regulated branch of the secretory pathway in yeast. J Cell Biol 140: 29-37.

70. Knop M, Strasser K (2000) Role of the spindle pole body of yeast in mediating assembly of the prospore membrane during meiosis. EMBO J 19: 3657-3667.

71. Straight AF, Belmont AS, Robinett CC, Murray AW (1996) GFP tagging of budding yeast chromosomes reveals that protein-protein interactions can mediate sister chromatid cohesion. Curr Biol 6: 1599-1608.

72. Michaelis C, Ciosk R, Nasmyth K (1997) Cohesins: Chromosomal Proteins that Prevent Premature Separation of Sister Chromatids. Cell 91: 35-45.

73. Shonn MA, McCarroll R, Murray AW (2002) Spo13 protects meiotic cohesin at centromeres in meiosis I. Genes Dev 16: 1659-1671.

74. Klapholz S, Esposito RE (1980) Isolation of *SPO12-1* and *SPO13-1* from a natural variant of yeast that undergoes a single meiotic division. Genetics 96: 567-588.

75. Lee BH, Amon A, Prinz S (2002) Spo13 regulates cohesin cleavage. Genes Dev 16: 1672-1681.

76. Katis VL, Matos J, Mori S, Shirahige K, Zachariae W, et al. (2004) Spo13 facilitates monopolin recruitment to kinetochores and regulates maintenance of centromeric cohesion during yeast meiosis. Curr Biol 14: 2183-2196.

77. Cao L, Alani E, Kleckner N (1990) A pathway for generation and processing of double-strand breaks during meiotic recombination in *S. cerevisiae*. Cell 61: 1089-1101.

78. Schwacha A, Kleckner N (1994) Identification of joint molecules that form frequently between homologs but rarely between sister chromatids during yeast meiosis. Cell 76: 51-63.

79. Hunter N, Kleckner N (2001) The single-end invasion: an asymmetric intermediate at the double-strand break to double-holliday junction transition of meiotic recombination. Cell 106: 59-70.

80. Börner GV, Kleckner N, Hunter N (2004) Crossover/noncrossover differentiation, synaptonemal complex formation, and regulatory surveillance at the leptotene/zygotene transition of meiosis. Cell 117: 29-45.

81. Tang S, Wu MKY, Zhang R, Hunter N (2015) Pervasive and essential roles of the Top3-Rmi1 decatenase orchestrate recombination and facilitate chromosome segregation in meiosis. Mol Cell 57: 607-621.

82. White EJ, Cowan C, Cande WZ, Kaback DB (2004) In vivo analysis of synaptonemal complex formation during yeast meiosis. Genetics 167: 51-63.

83. Carballo JA, Johnson AL, Sedgwick SG, Cha RS (2008) Phosphorylation of the axial element protein Hop1 by Mec1/Tel1 ensures meiotic interhomolog recombination. Cell 132: 758-770.

84. Penedos A, Johnson AL, Strong E, Goldman AS, Carballo JA, et al. (2015) Essential and Checkpoint Functions of Budding Yeast ATM and ATR during Meiotic Prophase Are Facilitated by Differential Phosphorylation of a Meiotic Adaptor Protein, Hop1. PLoS One 10: e0134297.

85. Herruzo E, Ontoso D, Gonzalez-Arranz S, Cavero S, Lechuga A, et al. (2016) The Pch2 AAA+ ATPase promotes phosphorylation of the Hop1 meiotic checkpoint adaptor in response to synaptonemal complex defects. Nucleic Acids Res 44: 7722-7741.

86. Garcia-Luis J, Clemente-Blanco A, Aragon L, Machin F (2014) Cdc14 targets the Holliday junction resolvase Yen1 to the nucleus in early anaphase. Cell Cycle 13: 1392-1399.

87. Grigaitis R, Susperregui A, Wild P, Matos J (2018) Characterization of DNA helicases and nucleases from meiotic extracts of *S. cerevisiae*. Methods Cell Biol 144: 371-388.

88. Mankouri HW, Ashton TM, Hickson ID (2011) Holliday junction-containing DNA structures persist in cells lacking Sgs1 or Top3 following exposure to DNA damage. Proc Natl Acad Sci U S A 108: 4944-4949.

89. Bzymek M, Thayer NH, Oh SD, Kleckner N, Hunter N (2010) Double Holliday junctions are intermediates of DNA break repair. Nature 464: 937-941.

90. Cromie GA, Hyppa RW, Taylor AF, Zakharyevich K, Hunter N, et al. (2006) Single Holliday junctions are intermediates of meiotic recombination. Cell 127: 1167-1178.

91. Liberi G, Maffioletti G, Lucca C, Chiolo I, Baryshnikova A, et al. (2005) Rad51-dependent DNA structures accumulate at damaged replication forks in sgs1 mutants defective in the yeast ortholog of BLM RecQ helicase. Genes Dev 19: 339-350.

92. Schwacha A, Kleckner N (1995) Identification of double Holliday junctions as intermediates in meiotic recombination. Cell 83: 783-791.

93. Attner MA, Miller MP, Ee LS, Elkin SK, Amon A (2013) Polo kinase Cdc5 is a central regulator of meiosis I. Proc Natl Acad Sci U S A 110: 14278-14283.

94. Argüello-Miranda O, Zagoriy I, Mengoli V, Rojas J, Jonak K, et al. (2017) Casein Kinase 1 Coordinates Cohesin Cleavage, Gametogenesis, and Exit from M Phase in Meiosis II. Developmental Cell 40: 37-52.

95. Geymonat M, Spanos A, Wells GP, Smerdon SJ, Sedgwick SG (2004) Clb6/Cdc28 and Cdc14 regulate phosphorylation status and cellular localization of Swi6. Mol Cell Biol 24: 2277-2285.

96. Leem SH, Chung CN, Sunwoo Y, Araki H (1998) Meiotic role of *SWI6* in *Saccharomyces cerevisiae*. Nucleic Acids Res 26: 3154-3158.

97. Kosugi S, Hasebe M, Tomita M, Yanagawa H (2009) Systematic identification of cell cycle-dependent yeast nucleocytoplasmic shuttling proteins by prediction of composite motifs. Proc Natl Acad Sci U S A 106: 10171-10176.

98. Petes TD, Botstein D (1977) Simple Mendelian inheritance of the reiterated ribosomal DNA of yeast. Proc Natl Acad Sci U S A 74: 5091-5095.

99. Smith AV, Roeder GS (1997) The yeast Red1 protein localizes to the cores of meiotic chromosomes. J Cell Biol 136: 957-967.

100. San-Segundo PA, Roeder GS (1999) Pch2 links chromatin silencing to meiotic checkpoint control. Cell 97: 313-324.

101. Vader G, Blitzblau HG, Tame MA, Falk JE, Curtin L, et al. (2011) Protection of repetitive DNA borders from self-induced meiotic instability. Nature 477: 115-119.

102. Pereira G, Manson C, Grindlay J, Schiebel E (2002) Regulation of the Bfa1p-Bub2p complex at spindle pole bodies by the cell cycle phosphatase Cdc14p. J Cell Biol 157: 367-379.

103. Pereira G, Schiebel E (2003) Separase regulates INCENP-Aurora B anaphase spindle function through Cdc14. Science 302: 2120-2124.

104. Imtiaz A, Belyantseva IA, Beirl AJ, Fenollar-Ferrer C, Bashir R, et al. (2018) CDC14A phosphatase is essential for hearing and male fertility in mouse and human. Hum Mol Genet 27: 780-798.

105. Longtine MS, McKenzie A, 3rd, Demarini DJ, Shah NG, Wach A, et al. (1998) Additional modules for versatile and economical PCR-based gene deletion and modification in *Saccharomyces cerevisiae*. Yeast 14: 953-961.

106. Padmore R, Cao L, Kleckner N (1991) Temporal comparison of recombination and synaptonemal complex formation during meiosis in *S. cerevisiae*. Cell 66: 1239-1256.

107. Carballo JA, Panizza S, Serrentino ME, Johnson AL, Geymonat M, et al. (2013) Budding yeast ATM/ATR control meiotic double-strand break (DSB) levels by down-regulating Rec114, an essential component of the DSB-machinery. PLoS Genet 9: e1003545.

108. Ahuja JS, Borner GV (2011) Analysis of meiotic recombination intermediates by two-dimensional gel electrophoresis. Methods Mol Biol 745: 99-116.

109. Newnham L, Jordan PW, Carballo JA, Newcombe S, Hoffmann E (2013) Ipl1/Aurora Kinase Suppresses S-CDK-Driven Spindle Formation during Prophase I to Ensure Chromosome Integrity during Meiosis. PLoS One 8: e83982.

Figure captions

Fig 1. *cdc14^{3HA}* behaves as a specific sporulation-deficient separation of function allele of *CDC14*. (A) Presence of *cdc14^{3HA}* does not perturb normal growth conditions when cultivated at 25°C, 30°C and 37°C in rich media (YPD). (B) Homozygous SK1 *cdc14^{3HA}* diploids do not form asci containing spores under standard conditions for sporulation. (C) *cdc14^{3HA}* diploid cells divide mitotically but lack di-tyrosine autofluorescence induced by UV light upon several days incubation in SPM media at 30°C. (D) FACS analysis of DNA content shows that *cdc14^{3HA}* cells complete meiotic DNA replication with identical kinetics as *CDC14* diploid cells. (E) *cdc14^{3HA}* cells undergo meiotic nuclear divisions at subtly slower, and lesser, frequencies than *CDC14* cells. Error bars represent the SEM over the mean values plotted.

Fig 2. Diminished protein levels in *cdc14^{3HA}* meiotic cells confer unsteady SPB integrity following meiotic divisions. (A) Diminished Cdc14 protein levels in wild-type (JCY902), and *cdc14* (JCY904) cells. Top panel shows immunodetection using a polyclonal α-Cdc14 (yE-17) and bottom panel using α-HA (12CA5). (*) denotes residual signal from earlier α-Cdc14 detection. *SMK1-3HA* expressed in same strain as *CDC14* or *cdc14^{3HA}*. (B) Quantification of protein levels shown in (A). (C) Staining of Spc29-CFP at SPBs, tubulin, and DNA, in wild-type (JCY892) and *cdc14^{3HA}* (JCY893) cells fixed at different stages of meiosis at 30°C. (D) *cdc14^{3HA}* cells develop meiosis I and II spindles with near wild-type kinetics. Lack of spore formation in *cdc14^{3HA}* meiotic cells is paralleled by loss of SPB's structural integrity.

Fig 3. Meiosis deficient *cdc14^{3HA}* mutant does not alter meiotic spindle's lifespan and dynamics. (A) Live-imaging of cells (GGY53 and GGY54) undergoing the first meiotic division carrying GFP-tubulin (red) and Spc29-CFP (green). (B) Visualization of spindle and SPB dynamics in cells (GGY53 and GGY54) undergoing the second meiotic division. For both A and B, at least four different positions were analyzed from two separate wells. A minimum of three time-courses per strain were run, acquired images were processed and movies generated (Supplementary Information). (C) Quantification of spindle's lifespan from cells undergoing MI or MII. Meiotic deficient *cdc14* cells (GGY54) present similar spindle dynamics when completing both meiotic divisions. Box plots depict median number of spindle's lifespan with whiskers representing upper and lower 1.5 interquartile range. Black dots represent outliers.

Fig 4. Missegregation occurs between sisters chromatids at MII in *cdc14^{3HA}* meiosis deficient mutant cells. (A) Top. Frequency of cells presenting connected DAPI masses at anaphase I. Bottom. Frequency of cells presenting connected nuclei at metaphase II. Meiotic deficient *cdc14* mutants (GGY54) present higher frequencies of unresolved nuclear divisions at late anaphase I and at metaphase II than wild type (GGY53). (B) Unequal distribution of Chromosome II-linked GFP homozygote markers at *lys2* locus in *cdc14* meiosis deficient mutant cells (JCY2330) denotes increased chromosome missegregation in comparison with wild-type cells (JCY2331). (C) Similar distribution of *CENIV*-linked GFP homozygote markers at *trp1* locus in *cdc14* meiosis deficient mutant cells (JCY2286) in comparison with wild-type cells (JCY2284) denotes correct homolog disjunction in anaphase I. (D) Unequal distribution of *CENIV-GFP* heterozygote markers in *cdc14* tetranucleated mutant cells (JCY2327) denotes increased sister chromatid missegregation in comparison with wild-type cells (JCY2326). (E) Meiotic defects in *cdc14^{3HA}* (JCY844) can be partly restored to wild-type levels (JCY840) by eliminating recombination (JCY2270/JCY2280) or bypassing second meiotic division (JCY2235/JCY2247). Statistical significance of differences was calculated by two-tailed *t* test, assuming unequal variances ($^{*}p < 0.05$; $^{**}p < 0.01$; $^{***}p < 0.001$; $^{****}p < 0.0001$; n.s.: not significant).

Fig 5. Meiotic recombination is impaired in *cdc14* meiotic deficient mutants. (A) Schematic description of the *HIS4-LEU2* hotspot (see text in result sections for more details). (B) *cdc14* meiotic deficient mutants (JCY2231) show increased levels of COs and ectopic recombination products after 12 hours in meiosis over the wild-type strain (JCY2232). (C) Quantification of DNA species, as described in [108], of southerns shown in (B) for both *CDC14* and $cdc14^{3HA}$ cells. (D) Schematic representation of DNA species commonly observed after analysing the *HIS4-LEU2* hotspot by 2D-gel electrophoresis. (E-F) Southern blots depicting 2D-gels at *HIS4-LEU2* hotspot in wild-type (JCY2232) and *cdc14* mutant (JCY2231) cells at different times during meiosis. (G) Quantification of DNA species observed in (E) and (F). Higher levels of mc-JMs characterize the lack of *cdc14* wild-type activity during meiosis.

Fig 6. Yen1 helps resolving aberrant recombination intermediates originated in the absence of Cdc14. (A) Multiple sequential time frames from a Zip1-GFP wild-type cell at 10 minutes interval displaying kinetics of SC assembling and disassembling. (B) Quantification of Zip1-GFP^{+} cells across the time in meiosis and normalized to the highest value for each strain. Absence of *cdc14* meiotic activity (GGY91) slows down progression into MI division. Presence of $Yen1^{ON}$ (JCY2164) further delays SC disassembling independently of Cdc14 activity (GGY92/GGY91). (C) Phosphorylation of Hop1 at T318 is not challenged by presence or absence of unresolved sister chromatids in *cdc14* meiosis deficient mutants (JCY844). (D) Analysis of expression levels and nuclease activity of Yen1 in *CDC14* (YJM7692) and $cdc14^{3HA}$ (YML7693) meiotic cells. Soluble extracts were prepared from *YEN1-Myc9* strains at 2-hr intervals after transfer into sporulation medium (SPM). Following anti-Myc immunoaffinity purification (IP), the IPs were analyzed by western blotting and tested for nuclease activity using Cy3-labeled Holliday junction DNA as a substrate. Upper panel: western blots of the cell extracts, with detection of Yen1-myc9, Cdc5, and Pgk1 (loading control). Lower panel: HJ resolution assay. The experiment shown is representative of two independent experiments. (E) Evolution of DNA content during meiotic S-phase from strains in (D). (F) Percentage of HJ cleavage in Yen1 IPs in the absence of *cdc14* meiotic activity. (G) Unrestrained resolution of recombination intermediates by $YEN1^{ON}$ aids sporulation in $cdc14^{3HA}$ cells (JCY2164). Frequency of asci containing one, two three and four spores when Yen1 is constitutively active in the absence of Cdc14 activity.

Fig 7. Model for *CDC14*-dependent resolution of complex recombination intermediates via multiple mechanisms. Contribution of Cdc14 to the correct disjunction of recombining chromosomes during meiosis. Early in prophase I, chromosomes initiate homologous recombination. 3'-resected ssDNA overhangs, invade an intact template with the help of recombinases. Displacement of intact strand from template allows the formation of D-loops, which can be stabilized allowing some DNA

synthesis. Next, stabilized branched DNA molecules might be disrupted by the action of the anti-recombinase heterotrimeric complex STR (Sgs1-Top3-Rmi1). Reannealing of the extended 3'-ssDNA overhang with the resected complementary strand, followed by further DNA synthesis will lead to the repair and ligation of the broken DNA duplex giving rise to a non-crossover via SDSA. The second end of the DSB can engage with the sister-chromatid at random leading to the formation of multi-chromatid JMs. Cdc14 helps minimizing the formation of these mc-JMs by an unknown mechanism. ZMM stabilization of JMs is ensued by the resolution of dHJs through the MutLγ interfering, class I, crossover pathway. Ndt80-dependent transcription, and activation, of Cdc5 triggers MutLγ resolvase activity. Unresolved linkages between bivalents that persist until anaphase I are mostly resolved by the action of the SSEs, Mus81-Mms4. Top3-Rmi1 as well as Cdc14 also contribute to the correct resolution of chromosomal entanglements between homologs during MI by unknown mechanisms. Residual chromatid intertwines between sister chromatids during the second meiotic division will be removed by the action of Yen1. The resolvase has been kept previously inactive by inhibitory phosphorylations until the second release of Cdc14 during anaphase II that dephosphorylates the resolvase promoting its full activation. See discussion for more details.

Supporting information captions

S1 Fig. Cdc14 is required during meiosis for correct nuclear division. (A) *cdc14^{3HA}* cells (JCY844) sustain both nuclear divisions although with subtly slower kinetics than wild type cells (JCY840) predominantly during the second round of nuclear segregation. (B) Quantification of cells with two and four nuclei as well as other aberrant nuclear structures during meiosis in *CDC14* (JCY840) and *cdc14^{3HA}* (JCY844) cells.

S2 Fig. Reduced levels of Cdc14 causes the sporulation defect observed in the mutant. (A) Sporulation efficiency of *cdc14^{3HA}* diploids transformed with multi-copy plasmid carrying MEN genes (GGY102/GGY103/GGY104/GGY105) and *cdc14^{3HA}* (GGY93). Only overexpression of the phosphatase rescues the sporulation defect. (B) Di-tyrosine autoflourescence of different mutant combinations as well as the control strains grown and sporulated on plates at 25°C and 30°C. *cdc14-1* homozygote diploids (JCY2353) sporulate at high efficiency under semi-permissive temperature forming preferentially tetrads whereas *cdc14^{3HA}* homozygote diploids will not sporulate at any temperature (JCY840). Combinations, and variable copy number, of the mutant genes can rescue the sporulation defect at different degrees (JCY2365/JCY2354/JCY2356).

S3 Fig. Meiotic *cdc14* mutant cells re-duplicate their SPBs and assemble both meiosis I, and II, spindles. (A) Images of fixed-cells at different time-points during synchronous parallel timecourses for both *CDC14* (JCY892) and *cdc14* mutant (JCY893) cells. *cdc14^{3HA}* cells initiate both meiotic divisions, as visualized using different fluorescence markers, whereas they do not complete sporulation. (B)

cdc14^{3HA} (JCY893) cells may display abnormal number of SPBs and atypical spindle conformations. (C) Terminal phenotype of a post-meiotic *cdc14*^{3HA} (JCY893) cell.

S4 Fig. Lack of Cdc14 in meiosis cause missegregation of chromosomes following both meiotic divisions. (A) Scheme depicting the chromosome GFP-tagging system placed at an interstitial *locus* within chromosome II (left) and at a centromere proximal *locus* within chromosome IV (right). (B) Representative images, and their frequencies, of the observed types of distribution of interstitial GFP dots in homozygosis in both mutant (JCY2230) and wild-type (JCY2231) meiotic cells. Cells were fixed in formaldehyde and nuclei strained with DAPI. Arrowheads indicate diffuse GFP in the nucleus. Bar=5µm.

S5 Fig. Lack of Cdc14 protein causes delays in synaptonemal complex disassembly. *cdc14*^{3HA} cells (GGY91) delayed their exit from pachytene compared to wild-type cells (GGY92), thus the higher accumulation of Zip1-GFP^{+} nuclei in the mutant compared to wild-type cells in spite of having initiated synapsis with similar kinetics. Error bars represent standard errors

S6 Fig. Spore formation is not prevented in the absence of Cdc14. (A) Representative images displaying the circular appearance of the pro-spore membrane component Don1-GFP following completion of both meiotic divisions in mutant (JCY904) and wild-type (JCY902) cells. (B) Western blot showing the meiotic kinetics of the protein Ssp1, subunit of the leading edge protein (LEP) complex (Ssp1-Ady3-Don1-Irc10) that establish a ring-like structure at the leading edge of the prospore membrane at meiosis II and it is required for spore formation in wild-type (JCY840) and mutant (JCY844) cells. (C) Western blot of the MAP Kinase Smk1, becoming highly phosphorylated in meiosis in both mutant (JCY904) and wild-type (JCY902) cells, which is representative of proficient sporulation potential.

S1 Table. *S. cerevisiae* strains used in this study. SK1 background strains were used throughout the study, unless specified otherwise.

S1 Video. Meiotic spindle's lifespan and dynamics in *CDC14* cells. Live imaging of cells (GGY53) undergoing both meiotic division carrying GFP-tubulin (red) and Spc29-CFP (green).

S2 Video. Meiotic spindle's lifespan and dynamics in *cdc14*^{3HA} cells. Live imaging of cells (GGY54) undergoing both meiotic division carrying GFP-tubulin (red) and Spc29-CFP (green).

S3 Video. Kinetics of synaptonemal complex assembly/disassembly in *CDC14* cells. Sequence of Zip1-GFP wild-type cells (GGY92) at 10 minutes interval displaying kinetics of SC assembling and disassembling.

S4 Video. Kinetics of synaptonemal complex assembly/disassembly in *cdc14^{3HA}* cells. Sequence of Zip1-GFP *cdc14^{3HA}* cells (GGY91) at 10 minutes interval displaying kinetics of SC assembling and disassembling.

Fig 1

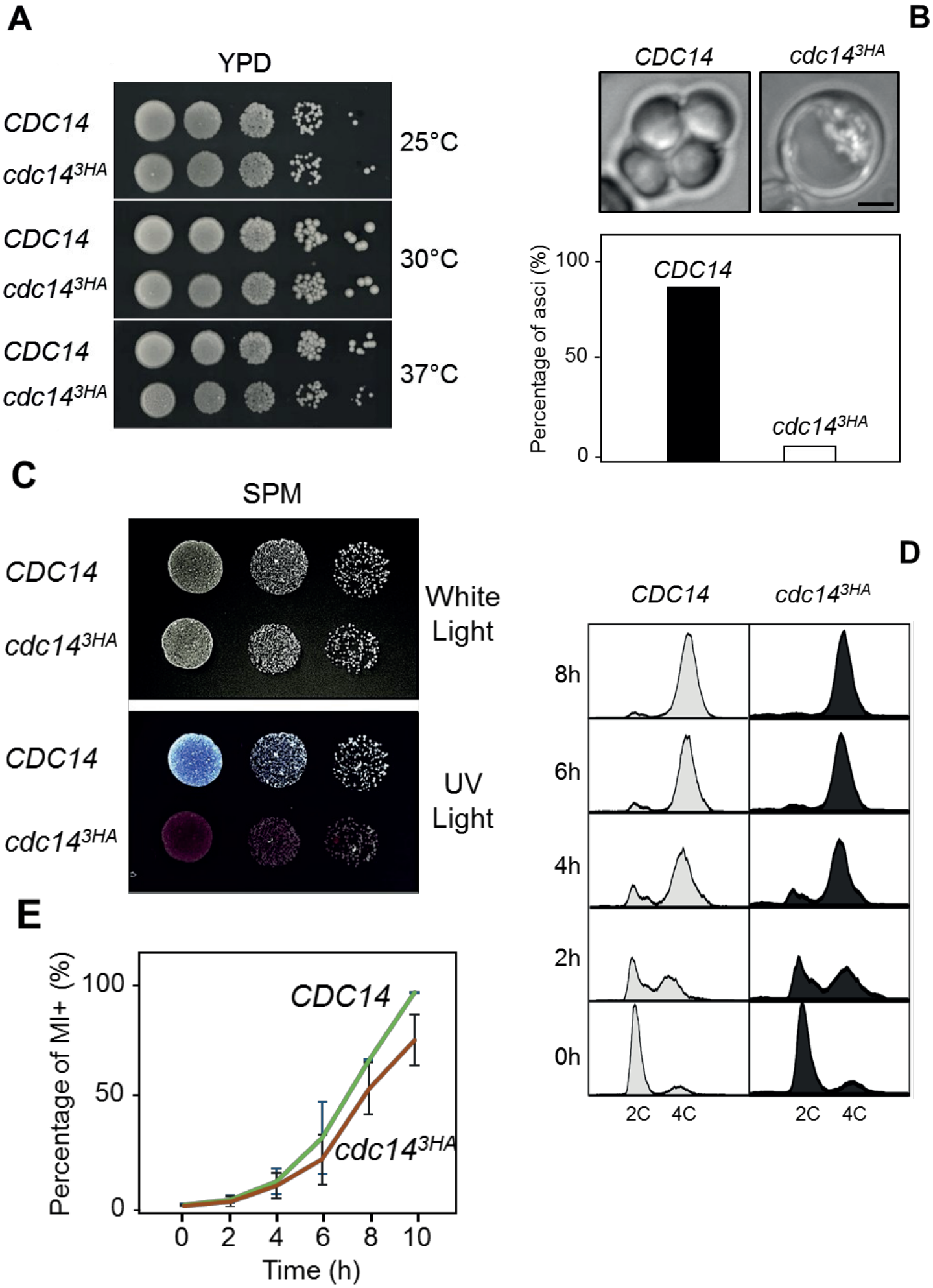
A
YPD
CDC14
cdc14^3HA
25°C
30°C
37°C
B
CDC14
cdc14^3HA
Percentage of asci (%)
100
50
0
C
SPM
White Light
UV Light
D
8h
6h
4h
2h
0h
2C
4C
E
Percentage of MI+ (%)
Time (h)
0
2
4
6
8
10

Fig 2

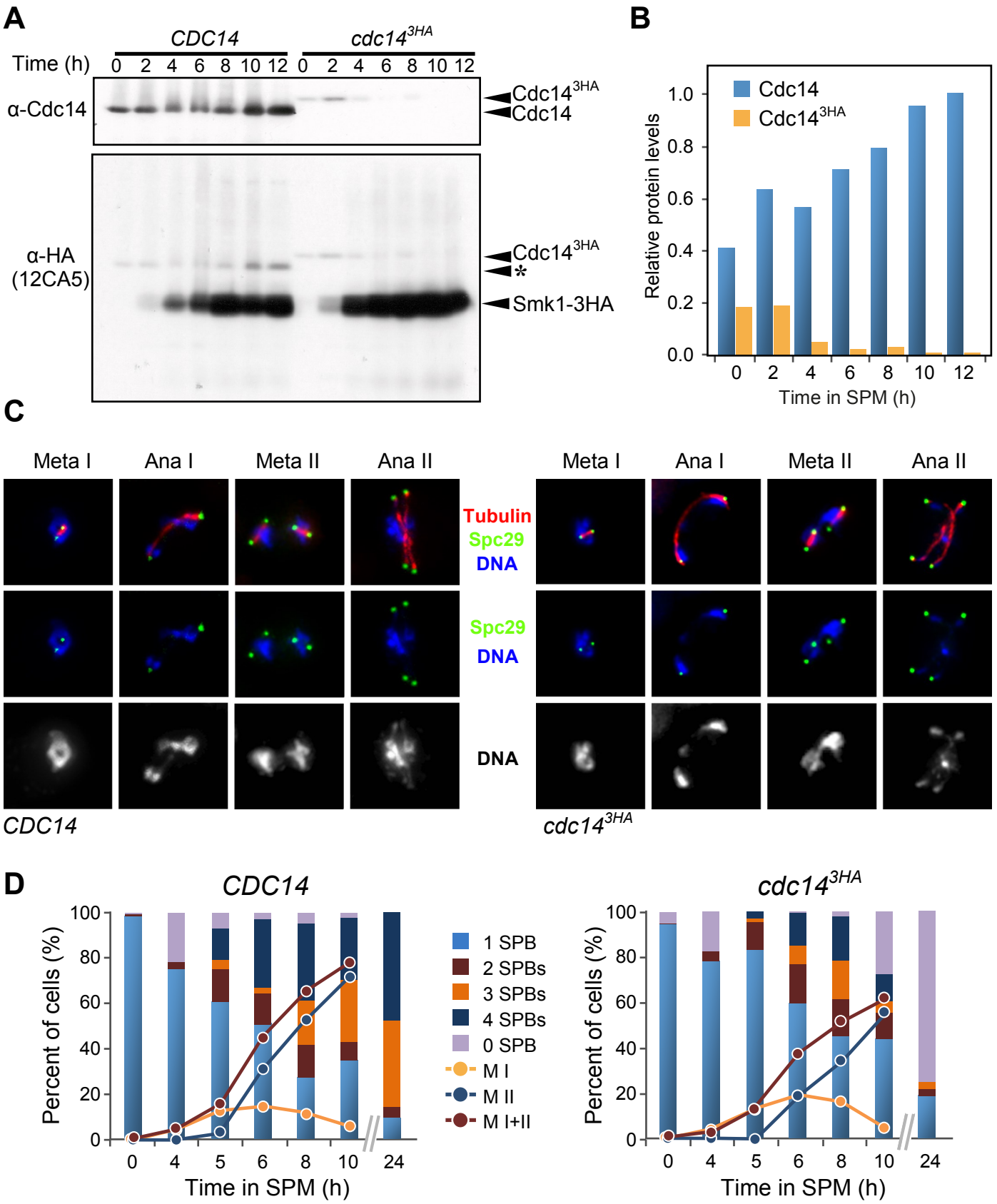
A
CDC14
cdc14^3HA
Time (h)
0 2 4 6 8 10 12 0 2 4 6 8 10 12
α-Cdc14
Cdc14^3HA
Cdc14
α-HA
(12CA5)
Cdc14^3HA
*
Smk1-3HA
B
Cdc14
Cdc14^3HA
Relative protein levels
1.0
0.8
0.6
0.4
0.2
0.0
0 2 4 6 8 10 12
Time in SPM (h)
C
Meta I
Ana I
Meta II
Ana II
Tubulin
Spc29
DNA
Spc29
DNA
DNA
CDC14
cdc14^3HA
D
CDC14
cdc14^3HA
Percent of cells (%)
100
80
60
40
20
0
0 4 5 6 8 10 24
Time in SPM (h)
1 SPB
2 SPBs
3 SPBs
4 SPBs
0 SPB
M I
M II
M I+II

Fig 3

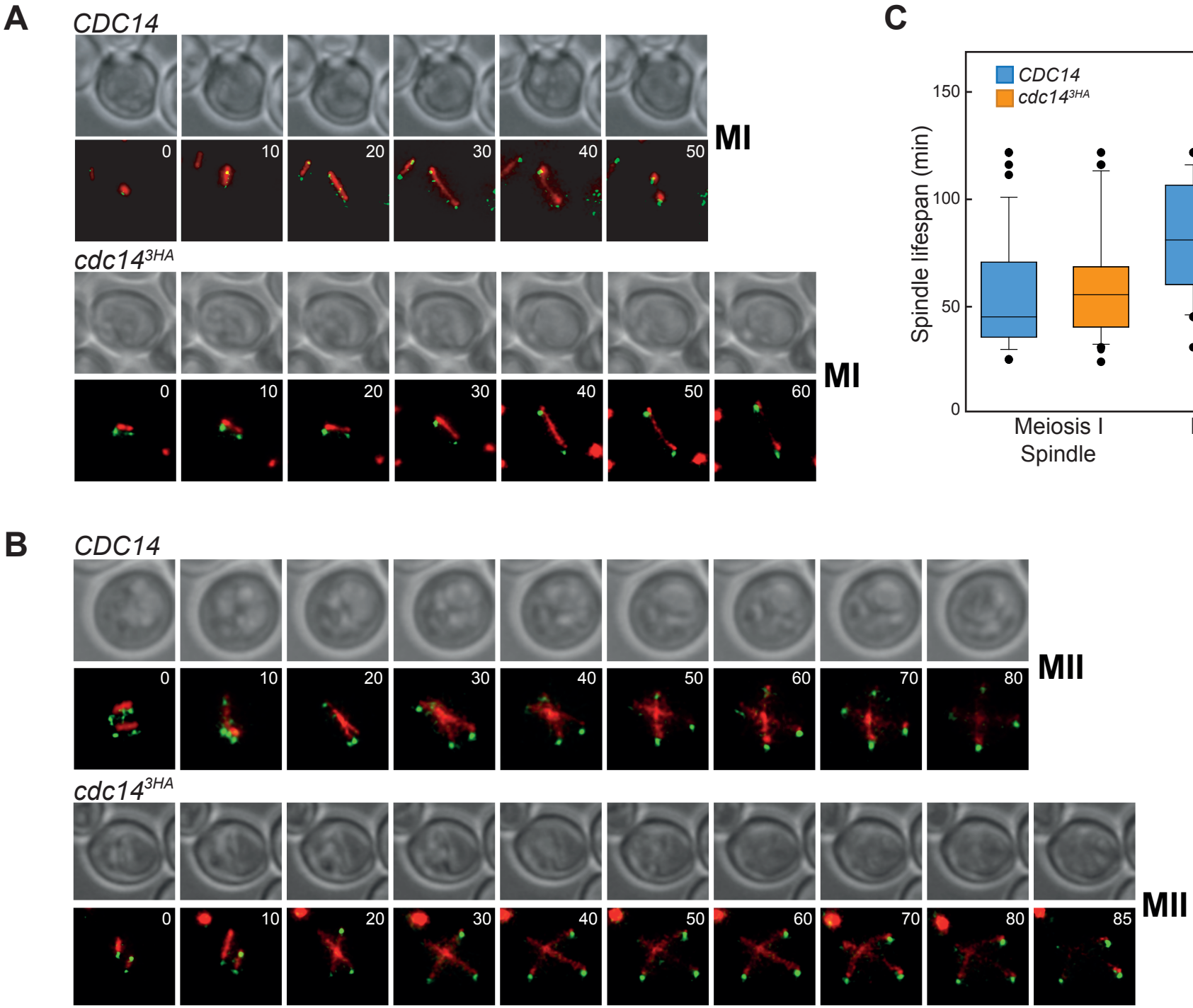
A
CDC14
0
10
20
30
40
50
MI
cdc14^3HA
0
10
20
30
40
50
60
MI
B
CDC14
0
10
20
30
40
50
60
70
80
MII
cdc14^3HA
0
10
20
30
40
50
60
70
80
85
MII
C
CDC14
cdc14^3HA
Spindle lifespan (min)
150
100
50
0
Meiosis I Spindle
Meiosis II Spindle

Fig 4

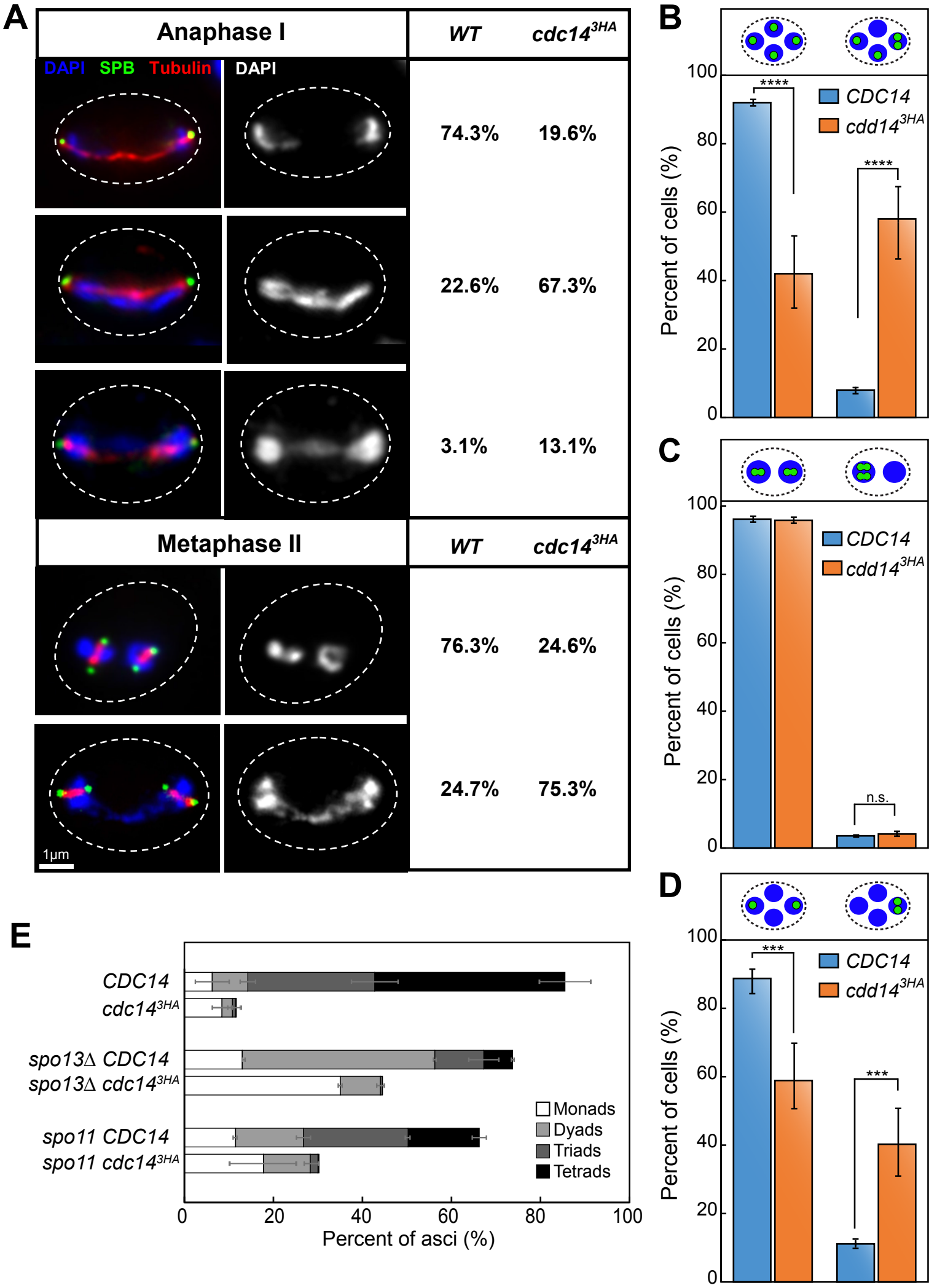
A
Anaphase I
WT
cdc14 3HA
DAPI SPB Tubulin
DAPI
74.3%
19.6%
22.6%
67.3%
3.1%
13.1%
Metaphase II
WT
cdc14 3HA
76.3%
24.6%
24.7%
75.3%
1µm
B
Percent of cells (%)
CDC14
cdd14 3HA
****
****
C
Percent of cells (%)
CDC14
cdd14 3HA
n.s.
D
Percent of cells (%)
CDC14
cdd14 3HA
***
***
E
CDC14
cdc14 3HA
spo13Δ CDC14
spo13Δ cdc14 3HA
spo11 CDC14
spo11 cdc14 3HA
Monads
Dyads
Triads
Tetrads
Percent of asci (%)

Fig 5

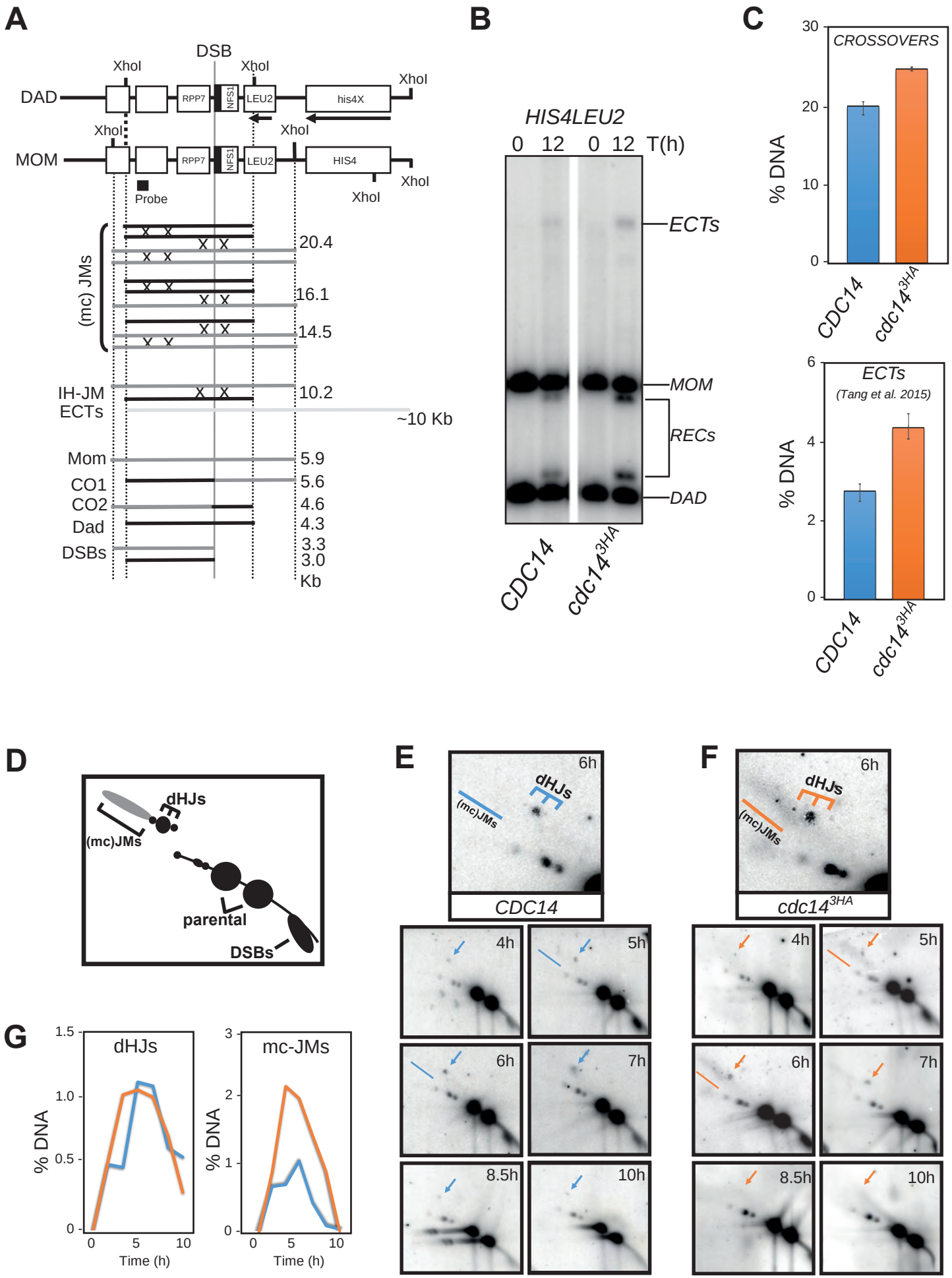
A
DSB
XhoI
DAD
MOM
RPP7
NFS1
LEU2
his4X
HIS4
Probe
(mc) JMs
20.4
16.1
14.5
IH-JM
ECTs
10.2
~10 Kb
Mom
CO1
CO2
Dad
DSBs
5.9
5.6
4.6
4.3
3.3
3.0
Kb
B
HIS4LEU2
0 12 0 12 T(h)
ECTs
MOM
RECs
DAD
CDC14
cdc14 3HA
C
CROSSOVERS
% DNA
ECTs
(Tang et al. 2015)
D
dHJs
(mc)JMs
parental
DSBs
E
6h
dHJs
(mc)JMs
CDC14
4h
5h
6h
7h
8.5h
10h
F
6h
dHJs
(mc)JMs
cdc14 3HA
4h
5h
6h
7h
8.5h
10h
G
dHJs
mc-JMs
% DNA
Time (h)

Fig 6

A

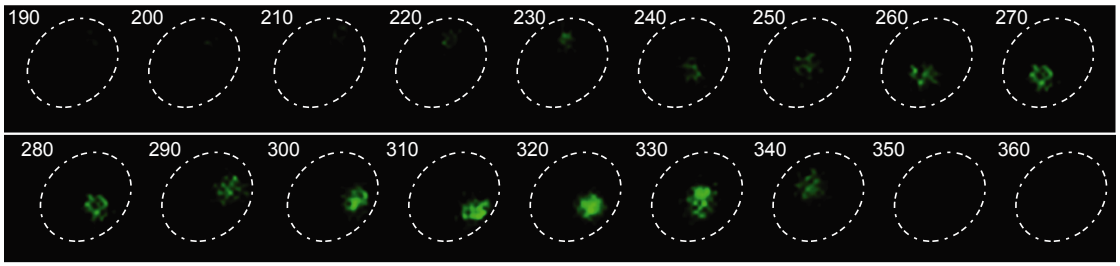

Zip1-GFP

B

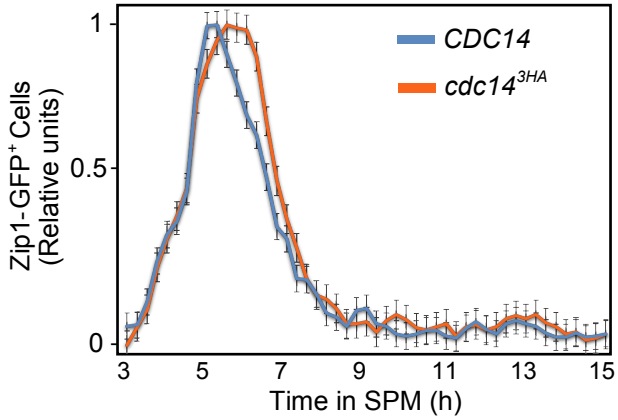

C

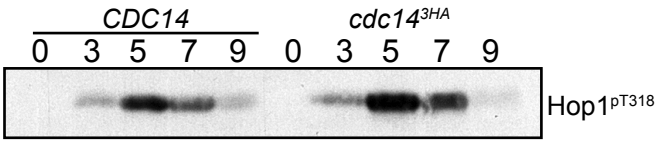

D

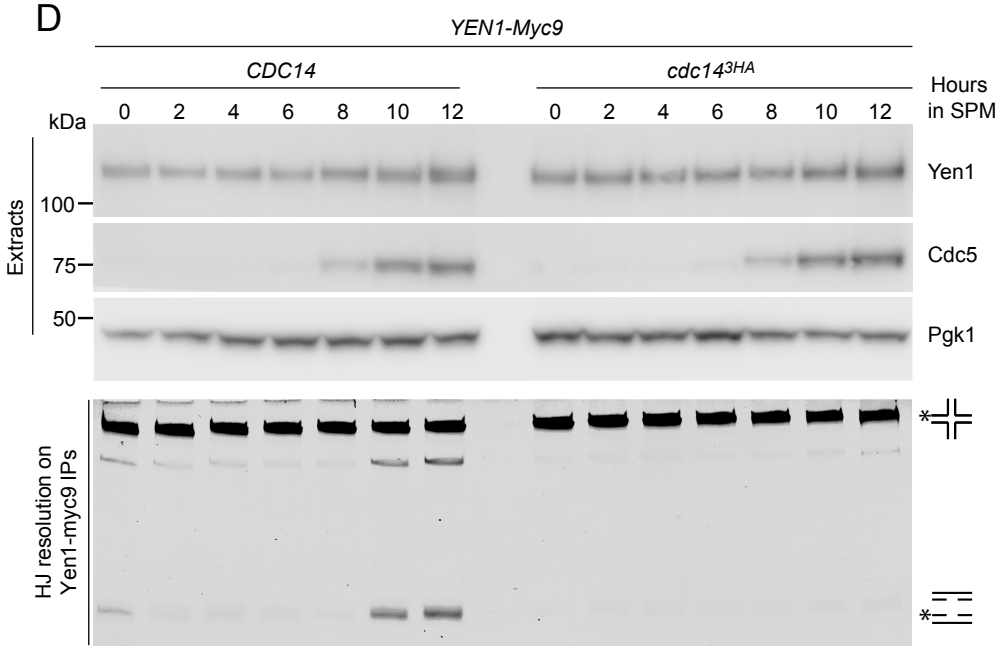

E

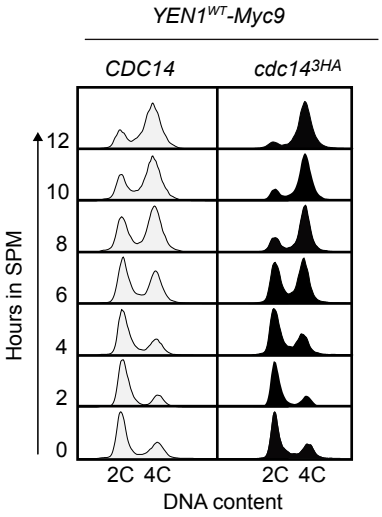

F

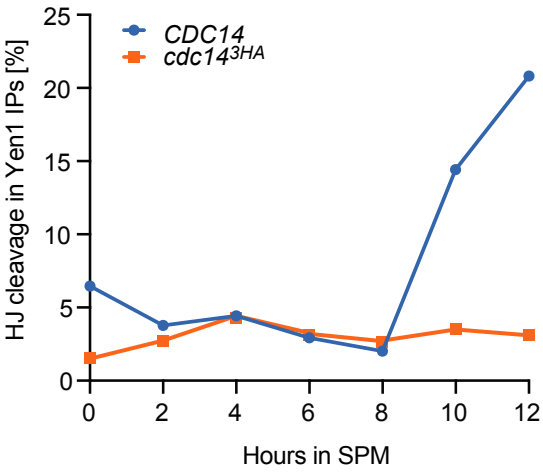

G

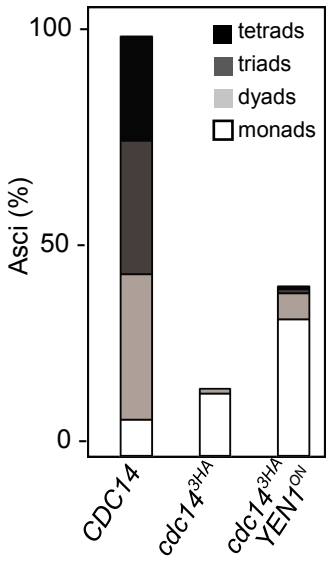

Fig 7

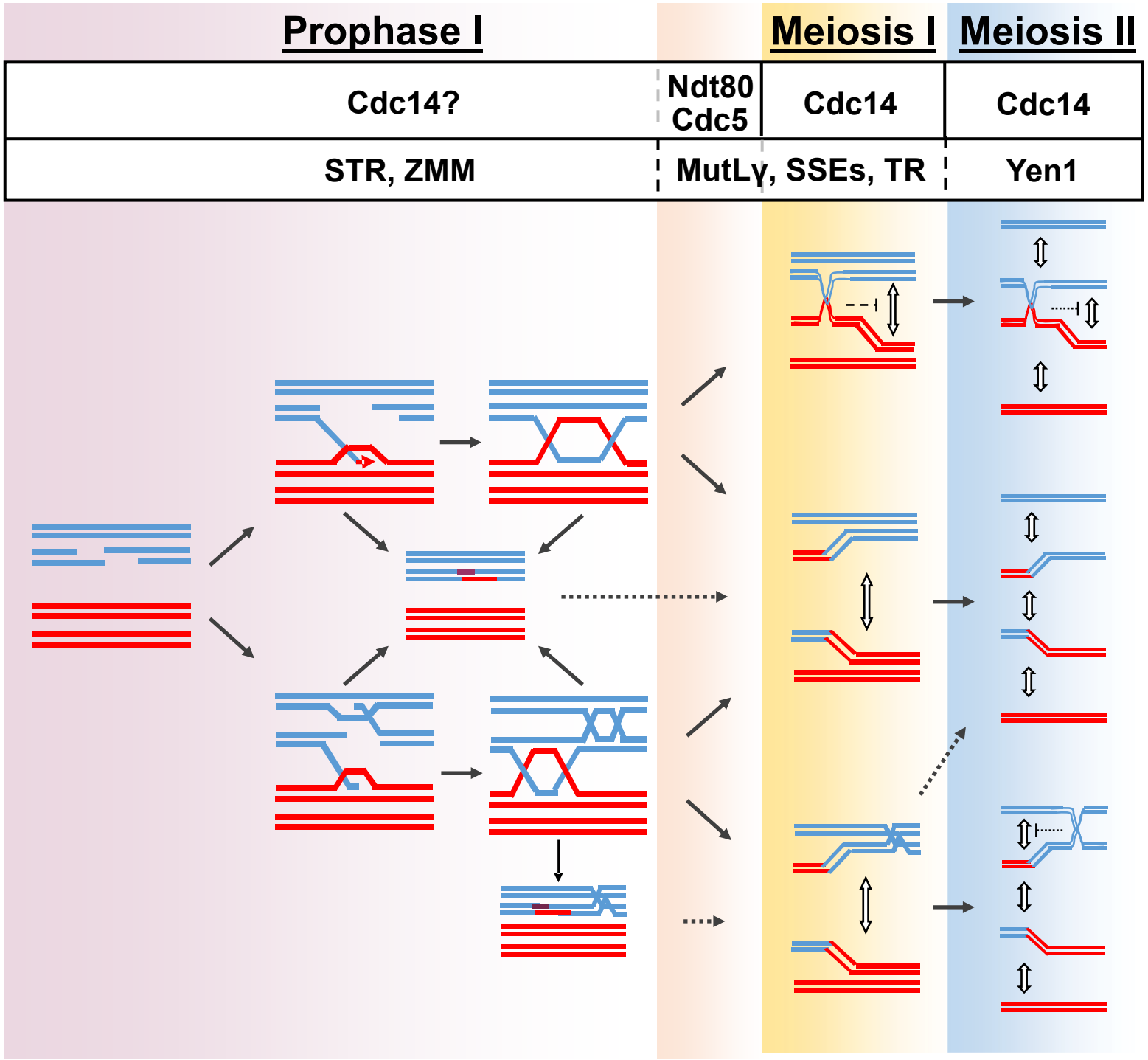
Prophase I
Meiosis I
Meiosis II
Cdc14?
Ndt80
Cdc5
Cdc14
Cdc14
STR, ZMM
MutLγ, SSEs, TR
Yen1

S1 Fig

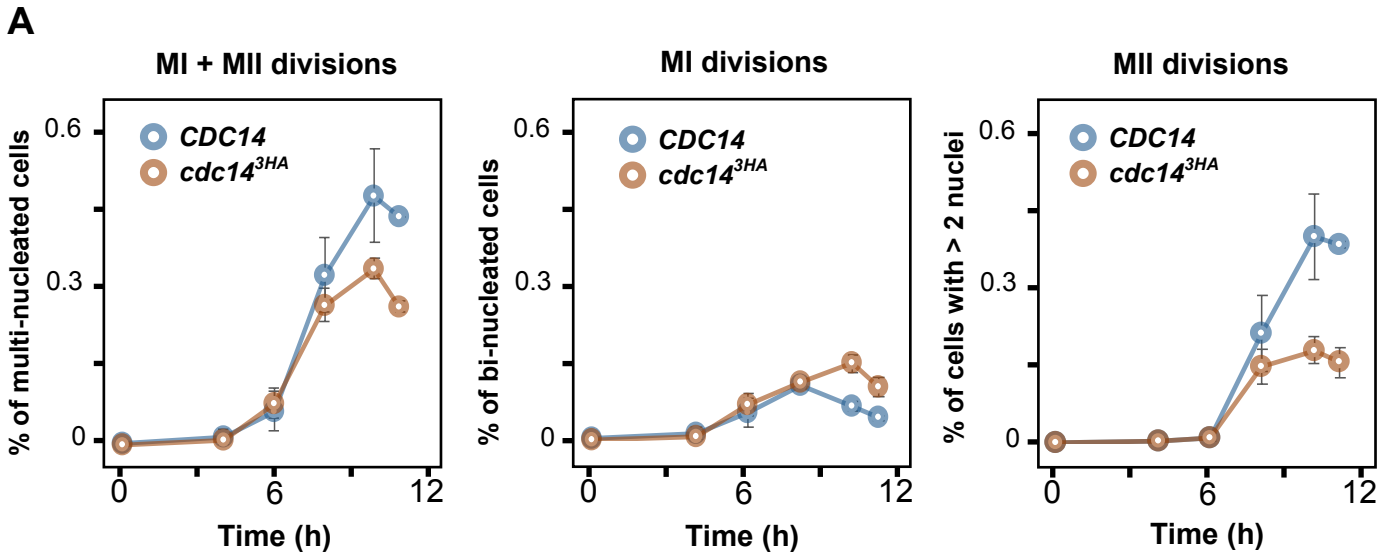
A
MI + MII divisions
MI divisions
MII divisions
CDC14
cdc14^3HA
% of multi-nucleated cells
% of bi-nucleated cells
% of cells with > 2 nuclei
0.6
0.3
0
0
6
12
Time (h)

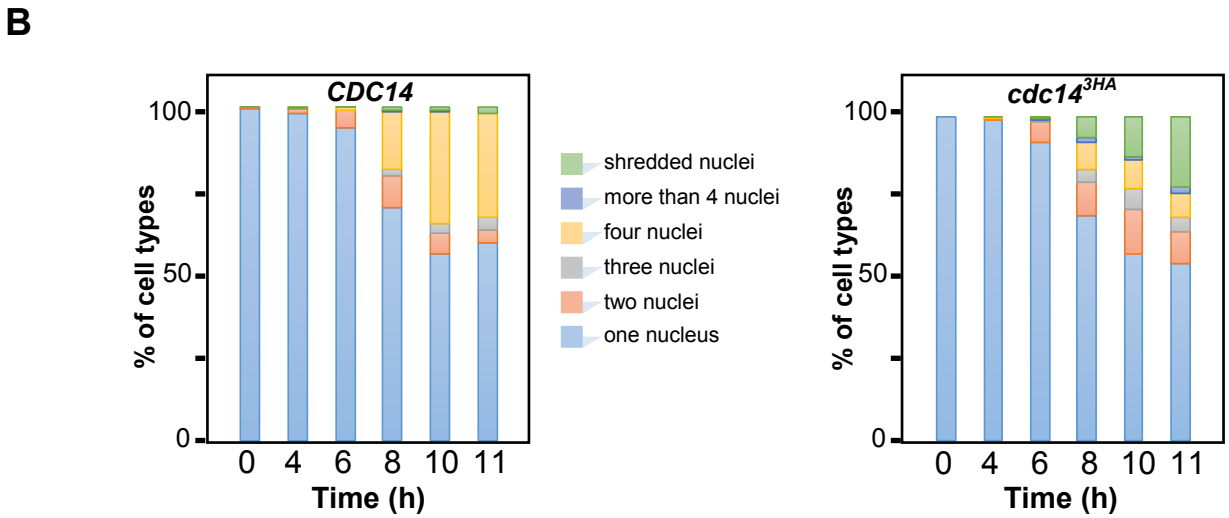
B
CDC14
cdc14^3HA
% of cell types
100
50
0
0 4 6 8 10 11
Time (h)
shredded nuclei
more than 4 nuclei
four nuclei
three nuclei
two nuclei
one nucleus

S2 Fig

A

Genotype		Sp. Efficiency
cdc14^{3HA} + 2μm (empty)		10.0%
cdc14^{3HA} + OX (*cdc14*^{3HA})		32.4%
cdc14^{3HA} + OX (*TEM1*^{3HA})		5.0%
cdc14^{3HA} + OX (*HA-CDC5*)		8.0%
cdc14^{3HA} + OX (*3HA-DBF2*)		7.6%
cdc14^{3HA} + OX (*CDC15*^{3HA})		10.6%
CDC14 + 2μm (empty)		62.8%

B

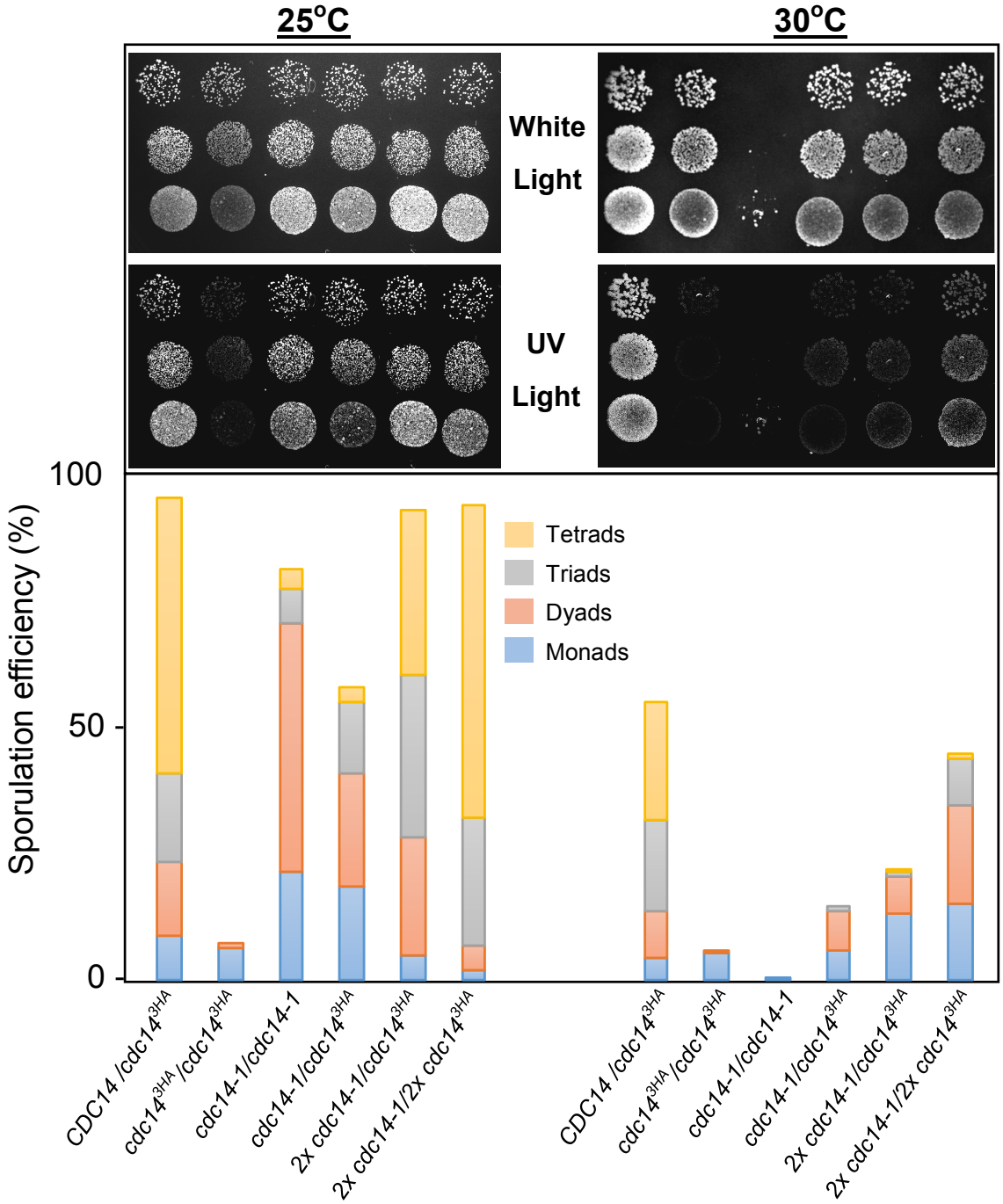

S3 Fig

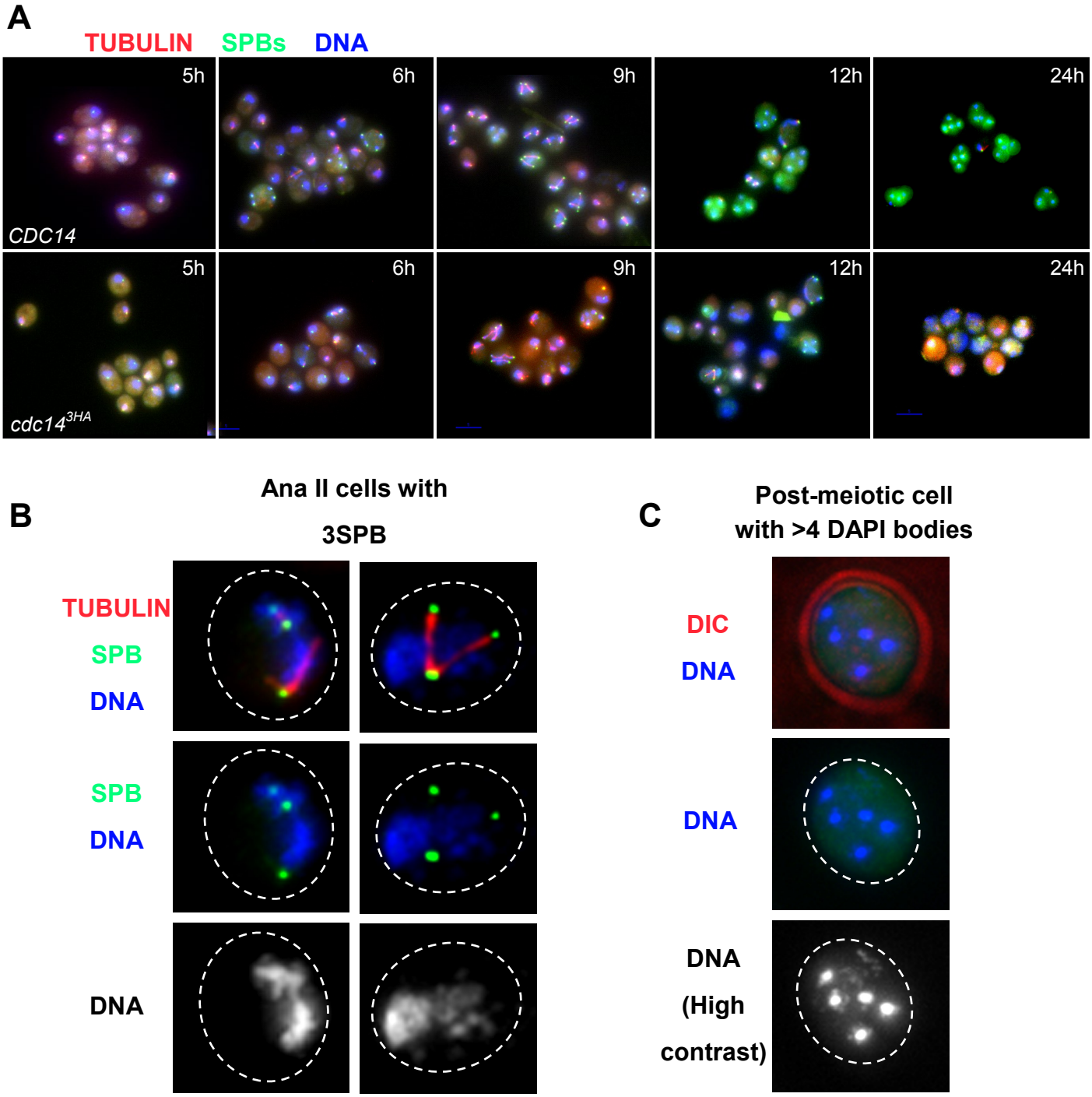
A
TUBULIN
SPBs
DNA
5h
6h
9h
12h
24h
CDC14
cdc14^{3HA}
B
Ana II cells with
3SPB
TUBULIN
SPB
DNA
SPB
DNA
DNA
C
Post-meiotic cell
with >4 DAPI bodies
DIC
DNA
DNA
DNA
(High
contrast)

S4 Fig

A

B

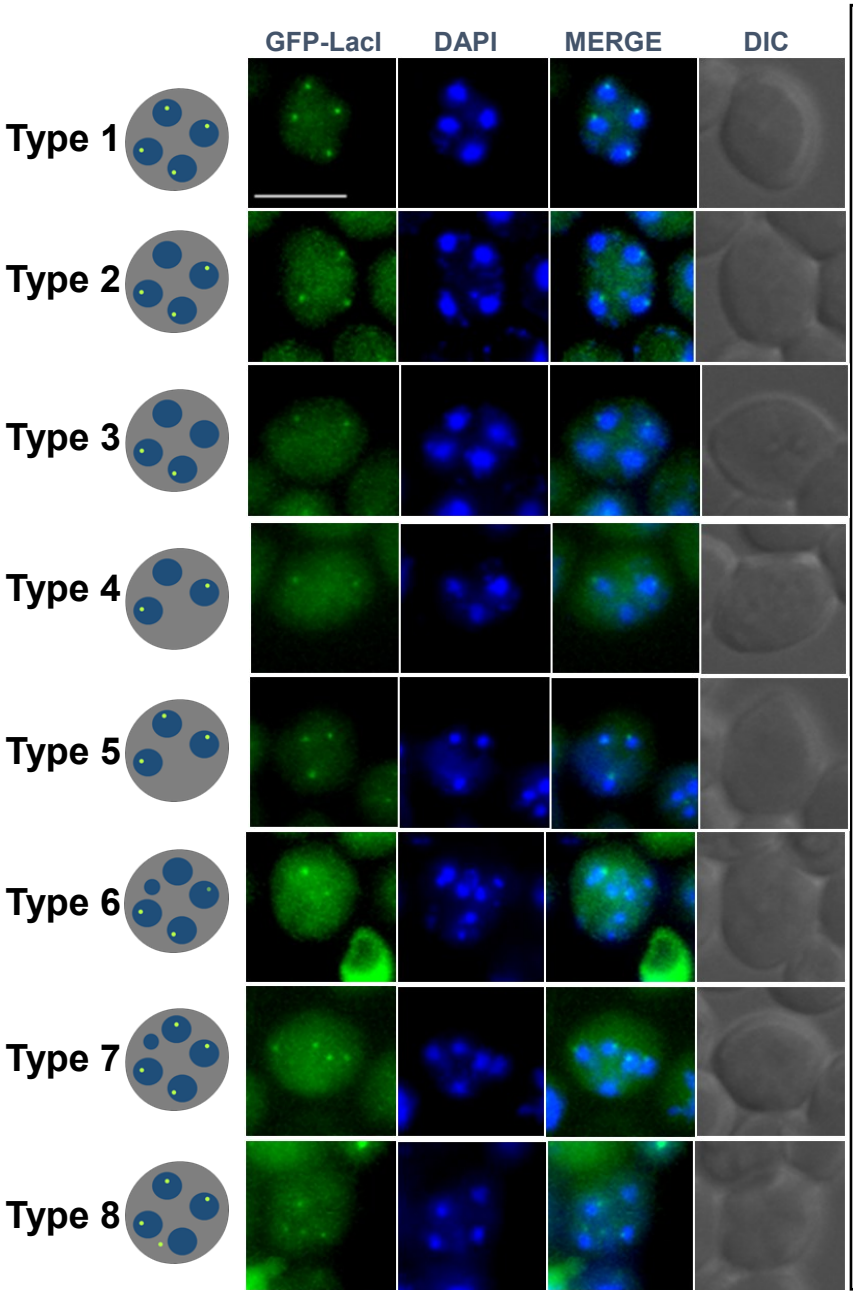

	ChrII (*lys2*)	
	CDC14	*cdc14*^{3HA}
Type 1	92.0%	42.4%
Type 2	2.4%	8.5%
Type 3	2.1%	3.3%
Type 4	0.3%	5.7%
Type 5	1.4%	13.2%
Type 6	0.3%	5.7%
Type 7	1.0%	14.5%
Type 8	0.5%	6.7%

S5 Fig

A

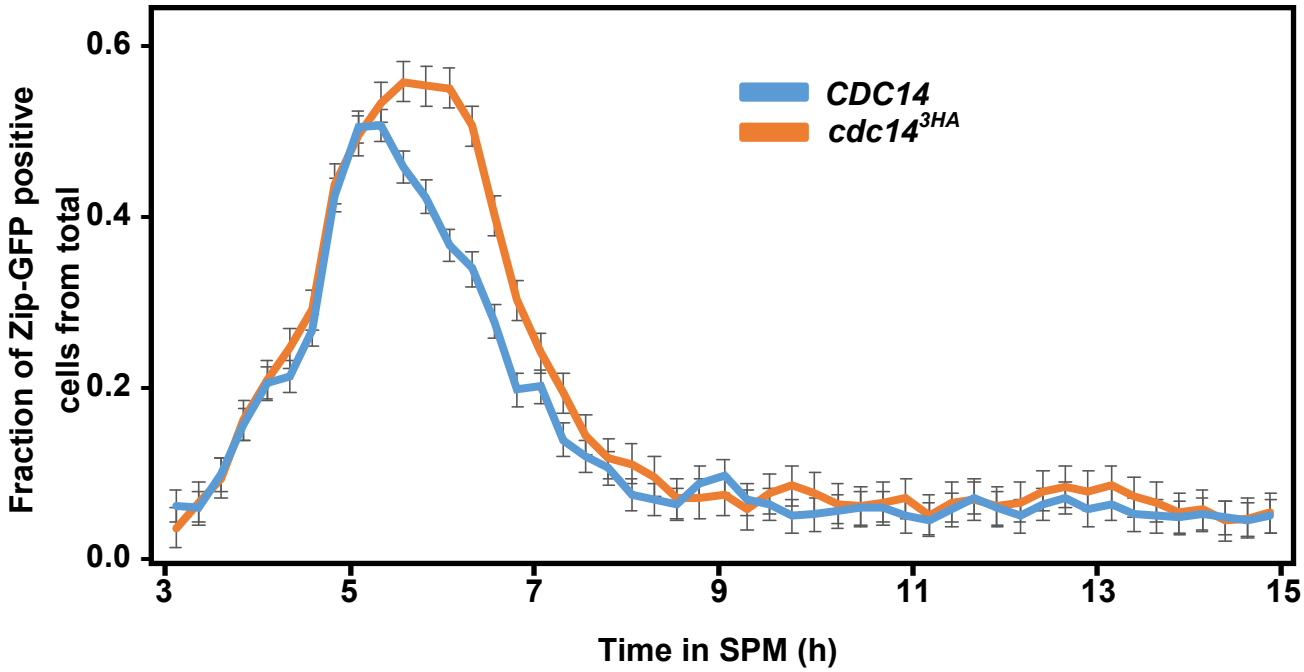
Fraction of Zip-GFP positive cells from total
0.0
0.2
0.4
0.6
3
5
7
9
11
13
15
Time in SPM (h)
CDC14
cdc14^3HA

B

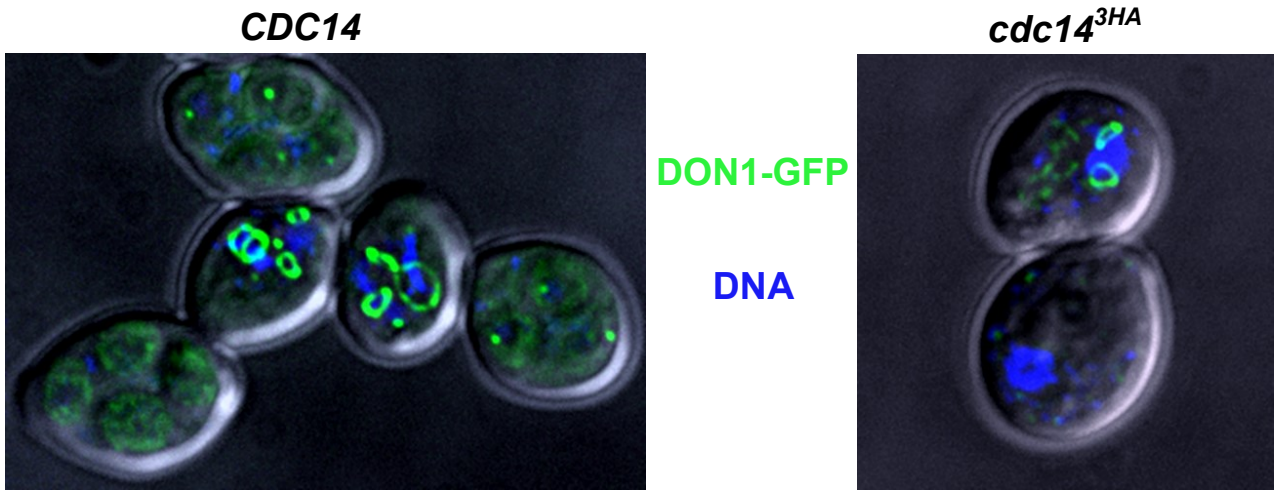
CDC14
cdc14^3HA
DON1-GFP
DNA

C

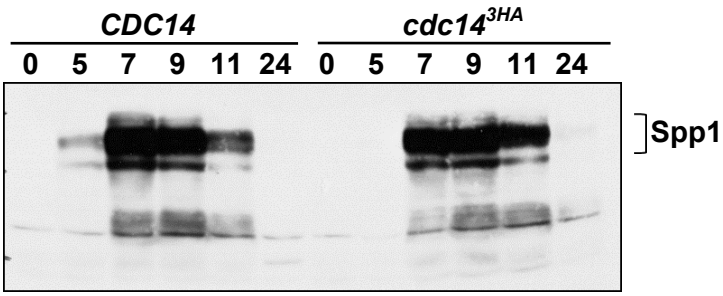
CDC14
cdc14^3HA
0 5 7 9 11 24 0 5 7 9 11 24
Spp1

D

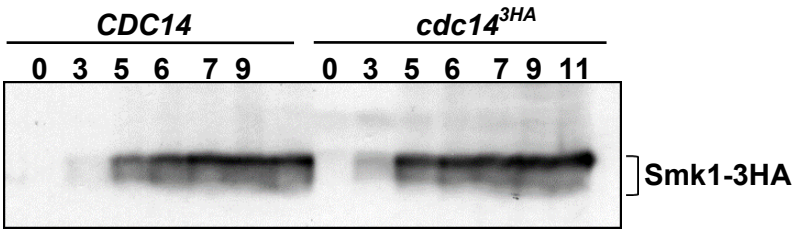
CDC14
cdc14^3HA
0 3 5 6 7 9 0 3 5 6 7 9 11
Smk1-3HA

Table S1. *S. cerevisiae* strains used in this study

Strain	Genotype
JCY840	*MAT a/α ho::LYS2/”, lys2/”, ura3/”, leu2::hisG/”, trp1::hisG/”, arg4-nsp/”, his4x/”*
JCY844	*MAT a/α ho::LYS2/”, lys2/”, ura3/”, leu2::hisG/”, trp1::hisG/”, arg4-nsp/”, his4x/”, cdc14^{3HA}::KanMX4/”*
GGY92	*MAT a/α ho::hisG/LYS2, lys2, ura3(Dsma-pst::hisG)/ura3, HIS4::LEU2-(NBam;ori)/his4x, Zip1-GFP(at AA700)/”, leu2::hisG/", cdc14^{3HA}::KanMX4/CDC14*
GGY91	*MAT a/α ho::hisG/LYS2, lys2, ura3(Dsma-pst::hisG)/ura3, HIS4::LEU2-(NBam;ori)/his4X or LEU2(NgomIV;ori)-URA3/his4x, Zip1-GFP(at AA700), leu2::hisG/", cdc14^{3HA}::KanMX4/"*
JCY902	*MAT a/α ho::hisG/”, ura3/”, leu2::hisG/+, lys2/”, trp1/”, SPC29-CFP::TRP1/”, DON1-dGFP-KanMX/”, pSMK1-3HA-URA3*
JCY904	As JCY902 but *cdc14^{3HA}::KanMX4/”*
GGY53	*MAT a/α ho::hisG/”, ura3/”, leu2::hisG/+, lys2/”, trp1/”, SPC29-CFP::TRP1/”, TUB-dGFP-URA3/”*
GGY54	*MAT a/α ho::hisG/”, ura3/”, leu2::hisG/+, lys2/”, trp1/”, SPC29-CFP::TRP1/”, TUB-dGFP-URA3/”, cdc14^{3HA}::KanMX4/”*
JCY2196	*MAT a/α ho::hisG/”, lys2/”, ura3/”, trp1/”, his4/”, leu2::hisG/”, cdc14^{3HA}::KanMX4/”*
JCY2235	*MAT a/α ho::LYS2/”, lys2/”, ura3/”, leu2::hisG/”, trp1::hisG/”, spo13Δ::URA3/”*
JCY2247	As JCY2235 but *cdc14^{3HA}::KanMX4/”*
JCY2270	*MAT a/α ho::LYS2/”, lys2/”, leu2::hisG/”, ura3/”, arg4-nsp/”, trp1::hisG/”, his4x/”, spo11-Y135F-HA::URA3/”*
JCY2280	As JCY2270 but *cdc14^{3HA}::KanMX4/”*
JCY2232	*MAT a/α ho::hisG/”, lys2/”, ura3(Δsma-pst::hisG)/”, leu2::hisG/”, his4X::LEU2-(NgoMIV;ori)-URA3/HIS4::LEU2-(NBam;ori)*
JCY2231	As JCY2232 but *cdc14^{3HA}::KanMX4/”*
YJM7692	*MATa/MATalpha ho::LYS2/” ura3/” leu2::hisG/” trp1::hisG/” his3::hisG/” YEN1-myc18::URA3/”*
YML7693	As YML3952 but *cdc143HA::KanMX4/”*

Table S1

JCY2164	*MAT a/α ho::LYS2/", lys2/", ura3/", leu2::hisG/", trp1/", his4x::LEU2-URA3/", YEN1-9A-myc18::URA3/", cdc14^{3HA}::KanMX4/", ZIP1-eGFP(at AA700)/"*
GGY93	JCY844 with pPD.2 (*CDC14HA3-URA3)*
GGY102	JCY844 with pSJ103 (*CDC15HA3-URA3)*
GGY103	JCY844 with pSJ57 (*HA3-DBF2-URA3)*
GGY104	JCY844 with pSJ56 (*TEM1HA3-URA3*)
GGY105	JCY844 with pSJ29 (*HACDC5-URA3*)
JCY2353	*MAT a/α ho::LYS2/", lys2/", his4x/", leu2::hisG/", ura3/", cdc14Δ::KanMX4/", trp1::cdc14-1::TRP1::LEU2/"*
JCY2365	*MAT a/α ho::LYS2/", lys2/", his4x/", leu2::hisG/", ura3/", cdc14Δ::KanMX4/CDC14^{3HA}::KanMX4, trp1::cdc14-1::TRP1::LEU2/trp1 arg4-nsp/ARG4*
JCY2354	*MAT a/α ho::LYS2/", lys2/", his4x/", leu2::hisG/", ura3/", cdc14^{3HA}::KanMX4/cdc14Δ::KanMX4, trp1::cdc14-1::TRP1::LEU2/"*
JCY2356	*MAT a/α ho::LYS2/", lys2/", his4x/", leu2::hisG/", ura3/", cdc14^{3HA}::KanMX4/cdc14^{3HA}::KanMX4, trp1::cdc14-1::TRP1::LEU2/"*
JCY2222	*MAT a/α ho::LYS2/", lys2/", ura3/", leu2::hisG/", his4/", Cyc1p-LacI-GFP-URA3/", trp1::LacO-TRP1 (at CENIV)/"*
JCY2224	As JCY2222 but *cdc14^{3HA}::KanMX4/"*
JCY2284	*MAT a/α ho::LYS2/", lys2/", ura3/", leu2::hisG/", his4/", Cyc1p-LacI-GFP-URA3/ura3, trp1::LacO-TRP1 (at CENIV)/trp1*
JCY2286	As JCY2284 but *cdc14^{3HA}::KanMX4/"*
JCY2251	*MAT a/α ho::LYS2/", his4/", trp1/", lys2::TetOx240:URA3/lys2, leu2::LEU2 tetR-GFP/leu2*
JCY2248	As JCY2251 but *cdc14^{3HA}::KanMX4/"*
JCY2331	*MAT a/α ho::LYS2/", his4/", trp1/", lys2::TetOx240:URA3/", leu2::LEU2 tetR-GFP/", CNM67-mCherry::natMX4/CNM67*
JCY2330	As JCY2331 but *cdc14^{3HA}::KanMX4/"*